Nuclear Gln3 Import Is Regulated by Nitrogen Catabolite Repression Whereas Export Is Specifically Regulated by Glutamine

Rajendra Rai,*,[1] Jennifer J. Tate,*,[1] Karthik Shanmuganatham,[†] Martha M. Howe,* David Nelson,* and Terrance G. Cooper*,[2]

*Department of Microbiology, Immunology and Biochemistry, University of Tennessee Health Science Center, Memphis, Tennessee 38163, and [†]Department of Infectious Diseases, St. Jude Children's Research Hospital, Memphis, Tennessee 38105

ABSTRACT Gln3, a transcription activator mediating nitrogen-responsive gene expression in *Saccharomyces cerevisiae*, is sequestered in the cytoplasm, thereby minimizing nitrogen catabolite repression (NCR)-sensitive transcription when cells are grown in nitrogen-rich environments. In the face of adverse nitrogen supplies, Gln3 relocates to the nucleus and activates transcription of the NCR-sensitive regulon whose products transport and degrade a variety of poorly used nitrogen sources, thus expanding the cell's nitrogen-acquisition capability. Rapamycin also elicits nuclear Gln3 localization, implicating Target-of-rapamycin Complex 1 (TorC1) in nitrogen-responsive Gln3 regulation. However, we long ago established that TorC1 was not the sole regulatory system through which nitrogen-responsive regulation is achieved. Here we demonstrate two different ways in which intracellular Gln3 localization is regulated. Nuclear Gln3 entry is regulated by the cell's overall nitrogen supply, *i.e.*, by NCR, as long accepted. However, once within the nucleus, Gln3 can follow one of two courses depending on the glutamine levels themselves or a metabolite directly related to glutamine. When glutamine levels are high, *e.g.*, glutamine or ammonia as the sole nitrogen source or addition of glutamine analogues, Gln3 can exit from the nucleus without binding to DNA. In contrast, when glutamine levels are lowered, *e.g.*, adding additional nitrogen sources to glutamine-grown cells or providing repressive nonglutamine nitrogen sources, Gln3 export does not occur in the absence of DNA binding. We also demonstrate that Gln3 residues 64–73 are required for nuclear Gln3 export.

KEYWORDS Gln3; nitrogen catabolite repression; nuclear export; nuclear import; glutamine; rapamycin; methionine sulfoximine

Gln3 is one of two GATA-family transcription activators that mediate nitrogen-responsive gene expression in *Saccharomyces cerevisiae* (Mitchell and Magasanik 1984a,b; Cooper *et al.* 1990; Stanbrough *et al.* 1995). One highly studied aspect of nitrogen-responsive regulation has centered on the regulated entry of Gln3 into the nucleus (Cooper 1982, 2004; Hofman-Bang 1999; Magasanik and Kaiser 2002; Broach 2012; Conrad *et al.* 2014). In nitrogen-rich repressive medium, Gln3 is effectively sequestered in the cytoplasm, thus ensuring that nitrogen catabolite repression (NCR)-sensitive transcription is restricted to low basal levels. This sequestration correlates with the existence of a Gln3-Ure2 complex (Drillien and Lacroute 1972; Drillien *et al.* 1973; Courchesne and Magasanik 1988; Blinder *et al.* 1Gln3996; Bertram *et al.* 2000; Kulkarni *et al.* 2001; Carvalho and Zheng 2003). When environmental supplies of readily usable nitrogen sources dwindle or only poorly used nitrogen sources are available or in times of short- or long-term nitrogen starvation, Gln3 dissociates from Ure2, enters the nucleus, and activates NCR-sensitive transcription. In addition to these three naturally occurring situations that trigger nuclear Gln3 localization, two additional methods of aberrantly achieving it in nitrogen-replete conditions exist: treating cells with the Target-of-rapamycin Complex 1 (TorC1) inhibitor rapamycin (Beck and Hall 1999; Cardenas *et al.* 1999; Hardwick *et al.* 1999; Bertram *et al.* 2000) or treating them with the glutamine synthetase inhibitor methionine sulfoximine (Msx) (Crespo *et al.* 2002; Tate *et al.* 2005; Kulkarni *et al.* 2006; Georis *et al.* 2011a).

doi: 10.1534/genetics.115.177725
Manuscript received April 28, 2015; accepted for publication August 31, 2015; published Early Online September 2, 2015.
[1]These authors contributed equally to this work.
[2]Corresponding author: Department of Microbiology, Immunology and Biochemistry, University of Tennessee Health Science Center, 858 Madison Avenue, Memphis, TN 38163. E-mail: tcooper@uthsc.edu

The requirements of TorC1 pathway–associated phosphatases for nuclear Gln3 localization and its response to rapamycin treatment established TorC1 as an important participant in Gln3 regulation (Di Como and Arndt 1996; Beck and Hall 1999; Cardenas *et al.* 1999; Hardwick *et al.* 1999; Jiang and Broach 1999; Bertram *et al.* 2000; Shamji *et al.* 2000; Jacinto *et al.* 2001; Crespo *et al.* 2002; Duvel *et al.* 2003; Wang *et al.* 2003; Yan *et al.* 2006). However, Gln3 control now appears to be more complex than the TorC1-mediated regulation originally envisioned. Intracellular Gln3 localization does not respond to leucine starvation or inhibitors of leucyl-transfer RNA (tRNA) synthetase, which downregulate TorC1, as reflected in hypophosphorylation of the TorC1 activity reporter Sch9 (Binda *et al.* 2009; Bonfils *et al.* 2012; Panchaud *et al.* 2013; Tate and Cooper 2013). Sch9 is a protein kinase that regulates protein synthesis and other cellular processes (Powers 2007; Urban *et al.* 2007). Further, cytoplasmic sequestration of Gln3 in a nitrogen-rich repressive medium, a condition that activates TorC1 kinase, does not require any of the components of the Gtr-Ego complexes required to activate TorC1 (Tate *et al.* 2015).

In addition to the dispensability of Gtr-Ego components required for TorC1 regulation, multiple previous observations support the conclusion that more than TorC1 activity is required for nitrogen-responsive Gln3 regulation (Cox *et al.* 2002, 2004a,b; Tate *et al.* 2006, 2009, 2010; Tate and Cooper, 2007; Georis *et al.* 2008, 2011a,b). In fact, five distinct physiological conditions that elicit nuclear Gln3 localization each possess unique protein phosphatase requirements (Tate and Cooper 2013). A response to rapamycin in excess nitrogen requires both Sit4 and PP2A. Nuclear Gln3 localization elicited by nitrogen limitation, *i.e.*, growth with a poorly used nitrogen source or short-term nitrogen starvation (~4–6 hr in the strains we analyzed), requires only Sit4, whereas responses to long-term nitrogen starvation (~6–10 hr in the strains we analyzed) or Msx treatment do not possess any known phosphatase requirements (Tate and Cooper 2013).

Specific alterations of the Gln3 molecule itself also support the existence of multiple regulatory pathways functioning in concert to affect nitrogen-responsive Gln3 control. First, substitution of serine residues in a putative Gln3 α-helix, $Gln3_{656–666}$, which disrupts the association of Gln3 with TorC1, only partially abolishes cytoplasmic Gln3 sequestration in nitrogen-replete medium (Rai *et al.* 2013), an expected characteristic when multiple regulatory pathways function in concert. Second, substitution of serine residues in another putative Gln3 α-helix, $Gln3_{583–591}$, abolished nuclear Gln3 localization in rapamycin-treated cells but did not affect Gln3 localization in repressed glutamine-grown nor derepressed proline-grown cells (Rai *et al.* 2014). These and most other previous studies have focused exclusively on regulated nuclear Gln3 entry. Only a single study addressed nuclear Gln3 export and reported the nuclear export signal to be Gln3 nuclear export sequence 336–345 ($NES_{336–345}$) based on the following observations: (1) elimination of Gln3 residues 336–345 in a truncated construct ($Gln3_{141–731}$) resulted in constitutively nuclear Gln3 in cells provided with a rich nitrogen supply, and (2) $Gln3_{141–731}$ interacted with Crm1 in a two-hybrid assay, but the interaction was lost on eliminating residues 336–345 (Carvalho and Zheng 2003). Finally, Gln3 residues 102–150 alone were shown to be necessary and sufficient to interact with Ure2 in a two-hybrid assay (Kulkarni *et al.* 2001; Carvalho and Zheng 2003). Wild-type Gln3 and a $Gln3_{1–200}$ peptide co-immunoprecipitated with Ure2, whereas co-immunoprecipitation of Gln3 lacking residues 1–101 was reduced (Carvalho and Zheng 2003).

In this work, we introduced amino acid substitutions into the previously identified Gln3 $NES_{336–345}$. During validation of that *gln3* mutant, we discovered that it failed to exhibit the phenotype expected from loss of the NES. Gln3 was nuclear when cells were grown in a variety of nitrogen-rich repressive media but not when glutamine itself was the sole nitrogen source or when cells were treated with glutamine analogues. We subsequently found that elimination of Gln3 residues 336–345 destroys the DNA-binding portion of the Gln3 zinc finger motif. This led us to search for and find a second sequence required for nuclear Gln3 export, residues 64–73. When these residues were abolished or altered, Gln3 was securely sequestered in the nucleus irrespective of the nitrogen source provided, including glutamine. These alterations did not, however, affect Gln3-Ure2 complex formation or Ure2 function. We further demonstrated that nuclear Gln3 export occurred in the absence of a functional Gln3 DNA binding domain when glutamine levels were high or cells were treated with glutamine analogues. In contrast, nuclear Gln3 export failed to occur in the absence of DNA binding when glutamine levels were lowered by adding additional nitrogen sources to glutamine-grown cells or providing non-glutamine repressive nitrogen sources. We conclude that the cell's overall nitrogen supply, *i.e.*, NCR, regulates Gln3 nuclear entry. In addition, glutamine levels themselves or a metabolite directly related to glutamine specifically determines whether DNA binding must occur before Gln3 can exit from the nucleus.

Materials and Methods

Strains and culture conditions

The *S. cerevisiae* strains we used are listed in Table 1. JK9-3da was the transformation recipient for *gln3* mutant plasmids except where otherwise indicated. A wild type rather than *gln3*Δ mutant was used as the transformation recipient to avoid pronounced secondary effects on multiple cellular processes known to occur in *gln3* loss-of-function mutants. Transformants, prepared by the lithium acetate method, were used as soon as possible after transformation (≤5 days).

Cultures (50 ml) were grown to mid-log phase (A_{600nm} = 0.5) in Difco Yeast Nitrogen Base (YNB, without amino acids or ammonia) minimal medium containing the indicated nitrogen source (final concentration 0.1%). Leucine (120 μg/ml), histidine (20 μg/ml), tryptophan (20 μg/ml),

Table 1 Strains used in this work

Strain	Pertinent genotype	Complete genotype
JK9-3da[a]	Wild type	*MAT***a**, *leu2-3,112*, *ura3-52*, *trp1*, *his4*, *rme1*, *HMLa*
TB50[b]	Wild type	*MAT***a**, *leu2-3*, *112*, *ura3-52*, *trp1*, *his3*, *rme1*, *HMLa*
TB123[b]	Wild-type Gln3-Myc^{13}	*MAT***a**, *leu2-3*, *112*, *ura3-52*, *trp1*, *his4*, *rme1*, *HMLa*, *GLN3-MYC^{13}[KanMX]*
FV007	*gln3*Δ, *gat1*Δ	(*MAT***a**, *gat1*Δ::*natMX*, *gln3*Δ::*kanMX*, *leu2-3*, *112*, *ura3-52*, *trp1*, *his4*, *rme1*, *HMLa*)
RR215	*ure2*Δ	*MAT***a**, *leu2-3,112*, *ura3-52*, *trp1*, *his4*, *rme1*, *HMLa,ure2*Δ::*kanMX*

[a] JK9-3d was constructed by Jeanette Kunz (Michael Hall's laboratory). Joseph Heitman isolated *MAT***a** and *MAT*α strains isogenic to JK9-3d by mating-type switching. JK9-3da is a hybrid strain containing contributions from the following strains: S288c, a strain from the Oshima Laboratory, and an unidentified strain from the Herskowitz Laboratory. It was chosen because of its robust growth, sporulation efficiency, and good growth on galactose (GAL$^+$). It may have a SUP mutation that allows translation through premature STOP codons and therefore produces functional alleles with many point mutations.

[b] JK9-3da is the parent of TB50, and TB50 is the parent of TB123.

and uracil (20 μg/ml) were added as needed to cover auxotrophic requirements. SC medium was prepared according to Tables 4 and 5 in Guthrie and Fink (1991). Casamino acids (CAA) medium consisted of YNB supplemented with the indicated nitrogen source(s) (final individual concentrations 0.1%) and 5 g/liter Difco Casamino Acids. Except in the case of rapamycin sensitivity, where indicated, cells were treated for 20 min with 200 ng/ml rapamycin or 30 min with 2 mM methionine sulfoximine (Msx), as described by Georis *et al.* (2011a). Glutamate-γ-hydroxamate (GAGM), diazo-oxo-norleucine (DON), azaserine (AZA), β-aspartate hydroxamate (βAsp), L-ethionine (LEth), methyl aspartate (MAsp), methyl-glutamate (MGlt), and Msx were added to cultures where indicated (final concentration 2 mM); cell samples then were collected after 30 min of treatment unless otherwise indicated.

Plasmid construction

All Gln3-Myc^{13} plasmids were constructed in *CEN*-based vectors using the primer sets in Table 2. Mutant constructs were produced using standard PCR-based methods (Rai *et al.* 2013, 2014). Plasmid pRR536 or one of its derivatives was used as template for PCR-based constructions. All plasmids contained full-length *GLN3* genes whose transcription was driven by its native wild-type promoter. The structures of all constructs were verified by restriction mapping and DNA sequence analyses.

Gln3-Myc^{13} localization

Cell collection and Gln3-Myc^{13} visualization by immunofluorescence staining were performed as described previously (Cox *et al.* 2002, 2004a,b; Tate *et al.* 2006, 2009; Georis *et al.* 2008). All cell images were collected as described previously (Tate *et al.* 2010; Rai *et al.* 2013, 2014).

Image processing

Microscopic image processing for presentation was achieved using Adobe Photoshop and Illustrator programs. Level settings (shadow and highlight only) were altered where necessary to avoid any change in or loss of cellular detail relative to that observed in the microscope; changes were applied uniformly to the image presented and were similar from one image to another. Midtone gamma settings were never altered. These processed images were used for illustrative presentation only, not for scoring Gln3-Myc^{13} intracellular distributions.

Determination of intracellular Gln3-Myc^{13} distributions

Gln3-Myc^{13} intracellular localizations were manually scored in 200 or more cells for each data point. Unaltered primary zvi image files viewed with Zeiss AxioVision 3.0 and 4.8.1 software were used exclusively for scoring purposes. Cells containing Gln3-Myc^{13} were classified into one of three categories: those in which Gln3-Myc^{13} was cytoplasmic (cytoplasmic fluorescent material only; red histogram bars), nuclear-cytoplasmic (fluorescent material appearing in both the cytoplasm and colocalizing with DAPI-positive material, DNA; yellow bars), or nuclear (fluorescent material colocalizing only with DAPI-positive material; green bars). Representative standard images of these categories appear in Figure 2 of Tate *et al.* (2009), along with descriptions of how the criteria were applied. The precision of our scoring has been documented repeatedly with a SD of under 10% for $N = 7$–10 experiments performed over 9 months in some cases and up to 3 years in others (Tate *et al.* 2006, 2010; Rai *et al.* 2013, 2014). Experiment-to-experiment variation can be assessed in this work by comparing data obtained with wild-type pRR536 transformants cultured in glutamine, glutamine + rapamycin, proline, ammonia, and ammonia + Msx because a separate wild-type culture accompanied each of the mutants.

Images for the accompanying histograms were chosen on the basis that they exhibited intracellular Gln3-Myc^{13} distributions as close as possible to those observed by quantitative scoring. However, identifying a field that precisely reflected the more quantitative scoring data was sometimes difficult unless Gln3 was situated in a single cellular compartment.

Co-immunoprecipitation of Gln3-Myc^{13} and NLS-LexA-Ure2 proteins

Cultures (50 ml) were grown to mid-log phase ($A_{600\text{nm}} = 0.5$) and harvested by flash freezing as described previously (Tate *et al.* 2005). Cells were resuspended in 300 μl of cold cell lysis buffer [50 mM Tris, pH 8, 150 mM NaCl, 5 mM EDTA, pH 8, 0.05% NP-40, 2 mM phenylmethylsulfonyl fluoride, and protease inhibitors (Complete Mini Protease Inhibitor Tablets, Roche)] and lysed with glass beads by vortexing, and the supernatant was clarified as described previously (Cox *et al.* 2004a), with the exception that the cells were vortexed eight times for 20- to 30-sec intervals with 30-sec cooling intervals on ice. A sample of the extract was removed for analysis prior

Table 2 Plasmids, primers, and oligonucleotides used in this work

Plasmid[a]	Residue alterations	Primer sets
pRR536	Wild-type $Gln3_{1–730}$-Myc^{13}	5′-CGCGGATCCTATACCAAATTTTAACCAATCCAATTCGTCAGCAATTGCT-3′ 5′-ATCCCCGCGGGACGTCAACTCCATAGAAGTGACTTTTCCG-3′
pRR658[b]	$Gln3_{NES\ mam.}$	5′-CAATCGGCCGCTGGAAAAGACCGCAGGCATTGCAAAGAGT-3 5′-ATCCCCGCGGGACGTCAACTCCATAGAAGTGACTTTTCCG-3′ 5′-CAATCGGCCGTCGGACGTTATCAAAAAGAGGATTTCAAAG-3 5′-CGCGGATCCTATACCAAATTTTAACCAATCCAATTCGTCAGCAATTGCT- 3′ 5′-GGCCGAATGAATTAGCCTTGAAATTAGCAGGTCTTGATATCAACAAGACAC-3′ 5′-GGCCGTGTCTTGTTGATATCAAGACCTGCTAATTTCAAGGCTAATTCATTC-3′
pRR702[b]	$Gln3_{10–20\Delta}$	5′-CAATCGGCCGCTTCGAATTTTCGGGGTCGTCTTGCATTTG-3′ 5′-CGCGGATCCTATACCAAATTTTAACCAATCCAATTCGTCAGCAATTGCT-3′ 5′-CAATCGGCCGCATGGTCGAAGTAATGAAGAGCCGAG-3′ 5′-ATCCCCGCGGGACGTCAACTCCATAGAAGTGACTTTTCCG-3′
pRR714[b]	$Gln3_{64–73\Delta}$	5′-CAATCGGCCGACGGACTTCGTGTCTCCTTTTACAGCAGC-3′ 5′-CGCGGATCCTATACCAAATTTTAACCAATCCAATTCGTCAGCAATTGCT-3′ 5′-CAATCGGCCGCATTGAGTCGAATGTGCCGCCGTTTAATCC-3′ 5′-ATCCCCGCGGGACGTCAACTCCATAGAAGTGACTTTTCCG-3′
pRR752[c]	$Gln3_{L64D,L67R,L71D,F73D}$-Myc^{13}	5′-CAATCGGCCGGATGATgacTATgacACGGACTTCGTG-3′ 5′-CGCGGATCCTATACCAAATTTTAACCAATCCAATTCGTCAGCAATTGCT-3′ 5′-CAATCGGccgTGCCTCgtcCATTGAGTCGAATGTGCCGCC-3′ 5′-ATCCCCGCGGGACGTCAACTCCATAGAAGTGACTTTTCCG-3′
pRR787	$Gln3_{L332D,L336D,M340D,L343D}$-Myc^{13}	5′-CAATCGGCCGatcGGTACCATGgtcTTTCTGGAAatcACCGCAGGCATTGCAAAGAG-3′ 5′-CGCGGATCCTATACCAAATTTTAACCAATCCAATTCGTCAGCAATTGCT-3′ 5′-CAATCGGCCGgacTCCTTAAAATCGGACGTTATCAAAAAG-3′ 5′-ATCCCCGCGGGACGTCAACTCCATAGAAGTGACTTTTCCG-3′
pRR1090[c]	$Gln3_{L64A,L67R,L71A,F73A}$-Myc^{13}	5′-CAATCGGCCGGATGATgcaTATgctACGGACTTCGTGTCTCC-3′ 5′-CGCGGATCCTATACCAAATTTTAACCAATCCAATTCGTCAGCAATTGCT-3′ 5′-CAATCGGccgTGCCTCtgcCATTGAGTCGAATGTGCCGCCG-3′ 5′-ATCCCCGCGGGACGTCAACTCCATAGAAGTGACTTTTCCG-3′
pRR1215	$Gln3_{M340D,L343D,L345D}$-Myc^{13}	5′-TTACATGGTACCgacAGGCCAgacTCCgacAAATCGGACGTTATCAAAAAG-3′ 5′-CGGAACAACAGATCTGGATGAAGATTTACTGGAACTTG-3′
pRR1217	$Gln3_{M340A,L343A,L345A}$-Myc^{13}	5′-TTACATGGTACCgcgAGGCCAgcaTCCgcaAAATCGGACGTTATCAAAAAG-3′ 5′-CGGAACAACAGATCTGGATGAAGATTTACTGGAACTTG-3′
DAL3-5	*DAL3* promoter oligonucleotide	5′-tcgacTGGATTGGCAAATAAATGGGGAAAGATAAGCGAGATAAGACTGATAAGAAG CATATGCGGTCTATTCATGg-3′ 5′-cCATGAATAGACCGCATATGCTTCTTATCAGTCTTATCTCGCTTATCTTTCCCCATT TATTTGCCAATCCAgtcga-3′
pAA15	NLS-LexA-URE2	Structure in Kulkarni *et al.* (2001)
pRS316	Vector	Structure in http://genome-www.stanford.edu/vectordb/vector_descrip/COMPLETE/PRS316.SEQ.html

[a] All plasmids contain full-length *gln3* genes driven by the native *GLN3* promoter.
[b] An *Eag*I site, encoding arginine and proline, replaced the deleted amino acids.
[c] The L67R substitution was required for the cloning strategy we employed.

to immunoprecipitation. Immunoprecipitaion of Myc- and/or LexA-tagged proteins was performed using the Immunoprecipitation Kit Dynabeads Protein G (Novex, Life Technologies). The remaining extract (200 μl) and 250 μl of cold cell lysis buffer were added to 50 μl of prewashed Dynabeads Protein G to which 5 μg of anti-Myc (9E10 Purified Anti-c-Myc, BioLegend) or anti-LexA (2–12) monoclonal mouse antibody (Santa Cruz Biotechnology) had been prebound (15 min at room temperature in the kit binding solution). After 15, 30, or 120 min of incubation at 4° with constant rotation, the immune-complex bead solution was divided in half, and the postbound supernatant was removed and frozen at −80°. The immune-complex beads were then washed three times with Dynabeads Kit washing buffer, resuspended in washing buffer, and transferred to a fresh microfuge tube, where the remaining wash solution was removed. The immunocomplexed beads were resuspended in SDS loading buffer, and the proteins were eluted by boiling and loaded onto a 6% SDS-PAGE gel for Western blot analysis. Western blot analyses were performed as described previously (Cox *et al.* 2004a); anti-Myc and anti-LexA antibodies were used at dilutions of 1:1000 and 1:200–400, respectively.

Electrophoretic mobility shift assays

Electrophoretic mobility shift assays (EMSAs) were performed as described previously (Kovari and Cooper 1991). ^{32}P-polynucleotide kinase–labeled oligonucleotide *DAL3-5* was used as the probe for DNA binding (Cunningham *et al.* 1996).

Quantitative RT-PCR analysis

Cultures (50 ml) were grown to mid-log phase (A_{600nm} = 0.45–0.5) in either 0.1% YNB-glutamine or proline medium and harvested by flash freezing (Tate *et al.* 2005). Total RNA

was extracted using the RNeasy Mini Kit (Qiagen), following the manufactures instructions for purification of total RNA from yeast—mechanical disruption of cells. Two modifications were made to this protocol: cells were broken with glass beads by vortexing, and on-column RNase-free DNase I treatment was performed for 40 min. Quality of the total RNA was analyzed on an Agilent 2100 Bioanalyzer using the Agilent RNA 6000 Nanochip by the University of Tennessee Health Science Center (UTHSC) Molecular Resource Center. Complementary DNAs (cDNAs) were generated using the Transcriptor First Strand cDNA Synthesis Kit (Roche) following the manufacturer's recommended protocol using both Oligo $(dT)_{18}$ and Random Hexamer primers for synthesis. Samples were prepared for quantification with LightCycler 480 SYBR Green I Master Mix (Roche) using the manufacturer's protocol. Quantification and subsequent analysis of cDNAs were performed on a Roche LightCycler 480 Real Time PCR System using LightCycler 480 software version 1.5. *GDH2* and *TBP1* primer sequences were as described previously (Georis *et al.* 2008, 2011a,b) .

Data availability

Strains and plasmids will be provided upon request, but only for non-commercial purposes. Commercial and commercial-development uses are prohibited. Materials provided may not be transferred to a third party without written consent.

Results

Gln3 sequence 336–345 is not demonstrably required for nuclear Gln3 export

This investigation began with the objective of constructing a mutant with constitutively nuclear Gln3-Myc^{13}. To achieve this, we introduced amino acid substitutions in the previously identified NES situated between Gln3 residues 336 and 345 (Carvalho and Zheng 2003) (Figure 1A). Deleting this sequence was previously shown to elicit constitutively nuclear Gln3-Myc^{9} localization, the expected phenotype of a NES mutant. Therefore, we substituted aspartate for four hydrophobic residues in and adjacent to the 336–345 sequence: Gln3$_{L332D,L336D,M340D,L343D}$-Myc^{13} (designated 332dddd Gln3, pRR787). These substitutions were made in a full-length wild-type *GLN3-MYC^{13}* gene controlled by its native promoter (pRR536) (Rai *et al.* 2013). Normal regulation of wild-type Gln3-Myc^{13} expressed from pRR536 has been well documented (Rai *et al.* 2013, 2014).

During validation of the newly constructed 332dddd Gln3-Myc^{13} mutant (pRR787), we made a surprising observation. 332dddd Gln3-Myc^{13} was not constitutively nuclear, as expected, when repressive glutamine or ammonia was provided as the sole nitrogen source (Figure 1, C and E, pRR787); 332dddd Gln3-Myc^{13} appeared to efficiently exit from the nucleus. In fact, with the exception of a slightly more nuclear response to rapamycin treatment, the substitution mutant strain exhibited more of a wild-type than mutant phenotype (Figure 1, C–E). Also noteworthy, 332dddd Gln3-Myc^{13} became highly nuclear in cells treated with Msx (Figure 1E).

Concerned that the L332D substitution adjacent to the putative NES had adversely affected its function, we made two additional mutants, substituting aspartate or alanine for three critical hydrophobic residues in the putative NES itself: Gln3$_{M340D,L343D,L345D}$-Myc^{13} (designated 340ddd Gln3-Myc^{13}, pRR1215) and Gln3$_{M340A,L343A,L345A}$-Myc^{13} (designated 340aaa Gln3-Myc^{13}, pRR1217). Neither mutant exhibited constitutive nuclear Gln3-Myc^{13} localization in glutamine or ammonia medium (Figure 2, A and C). There was a slight cytoplasmic shift in glutamine-grown 340aaa Gln3-Myc^{13}–containing cells treated with rapamycin (Figure 2A), but otherwise both mutants were virtually wild type in glutamine-, proline- or ammonia-grown cells irrespective of whether or not they were treated with Msx (Figure 2, A–C).

These data suggested one of two possibilities: (1) Gln3 sequence 336–345 was not responsible for nuclear Gln3 export, reopening the question of where the functioning NES for Gln3 was located, or (2) there was more than one functional Gln3 NES that could account for the wild-type phenotype of the *gln3* amino acid substitutions in pRR1215 (340ddd Gln3-Myc^{13}) and pRR1217 (340aaa Gln3-Myc^{13}). Our task was to distinguish between these possibilities.

To avoid being misled during a search for potential Gln3 NESs, we determined baseline Gln3-Myc^{13} export supported by a well-characterized NES by replacing Gln3 residues 336–345 with the mammalian protein kinase inhibitor (PKI) NES (designated NES mam. Gln3, pRR658) (Wen *et al.* 1994; Görner *et al.* 2002). This heterologous NES resulted in complete cytoplasmic localization of Gln3 irrespective of the nitrogen source provided, TorC1 status of the cell, or Msx inhibition of glutamine synthetase (Figure 2, pRR658). One interpretation of these results was that if nuclear Gln3 export were sufficiently active, it could overcome nuclear Gln3 entry that occurred during growth in derepressive conditions, *i.e.*, with proline as the nitrogen source, or in cells treated with rapamycin or Msx (Figure 2, pRR1215 or pRR1217). It alternatively suggested that nuclear Gln3 export mediated by the native Gln3 NES differed from that mediated by the PKI NES. The pertinent observation here was that replacing the Gln3 NES with the PKI NES was the first among many Gln3 alterations, other than destruction of nuclear localization sequences, where Gln3 failed to relocate to the nucleus after treating cells with Msx. By inductive reasoning, this result also suggested that nuclear export of wild-type Gln3 was regulated and that this regulation was lost when residues 336–345 were replaced.

Identification of a Gln3 sequence with the characteristics of a NES

To identify additional candidate sequences potentially participating in nuclear Gln3 export, we analyzed the Gln3 sequence using several NES prediction programs, including the NetNES 1.1 Server (http://www.cbs.dtu.dk/services/NetNES/) (la Cour

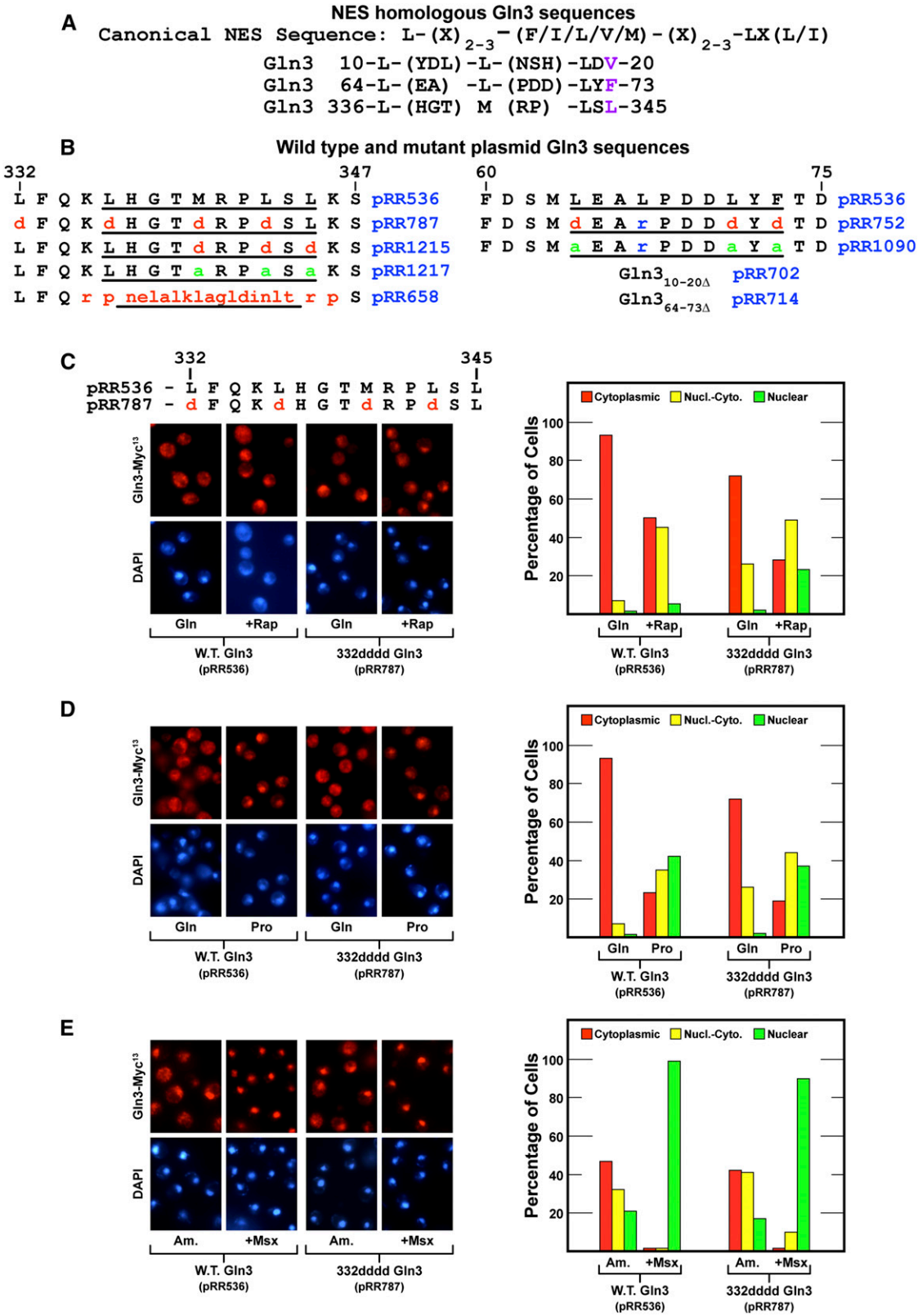

Figure 1 (A) Amino acid sequences of wild-type Gln3 that are homologous with the canonical NES in the sequence used by Carvalho and Zheng (2003). (B) Wild-type (pRR536) and substitution mutant plasmid sequences of Gln3 regions homologous with NESs. Gln3 amino acid coordinates appear above the sequences. (C–E) Gln3-Myc^{13} export is not demonstrably affected by amino acid substitutions in and adjacent to the previously reported Gln3 NES. Wild-type (pRR536) and Gln3$_{L332D,L336D,M340D,L343D}$-Myc^{13} (pRR787) mutant cells were grown in YNB-glutamine (C and D, Gln), YNB-proline (D, Pro), or YNB-ammonia (E, Am) medium to mid-log phase (A_{600nm} = 0.5). Samples were removed for assay of Gln3-Myc^{13} localization. Rapamycin (C, +Rap) or

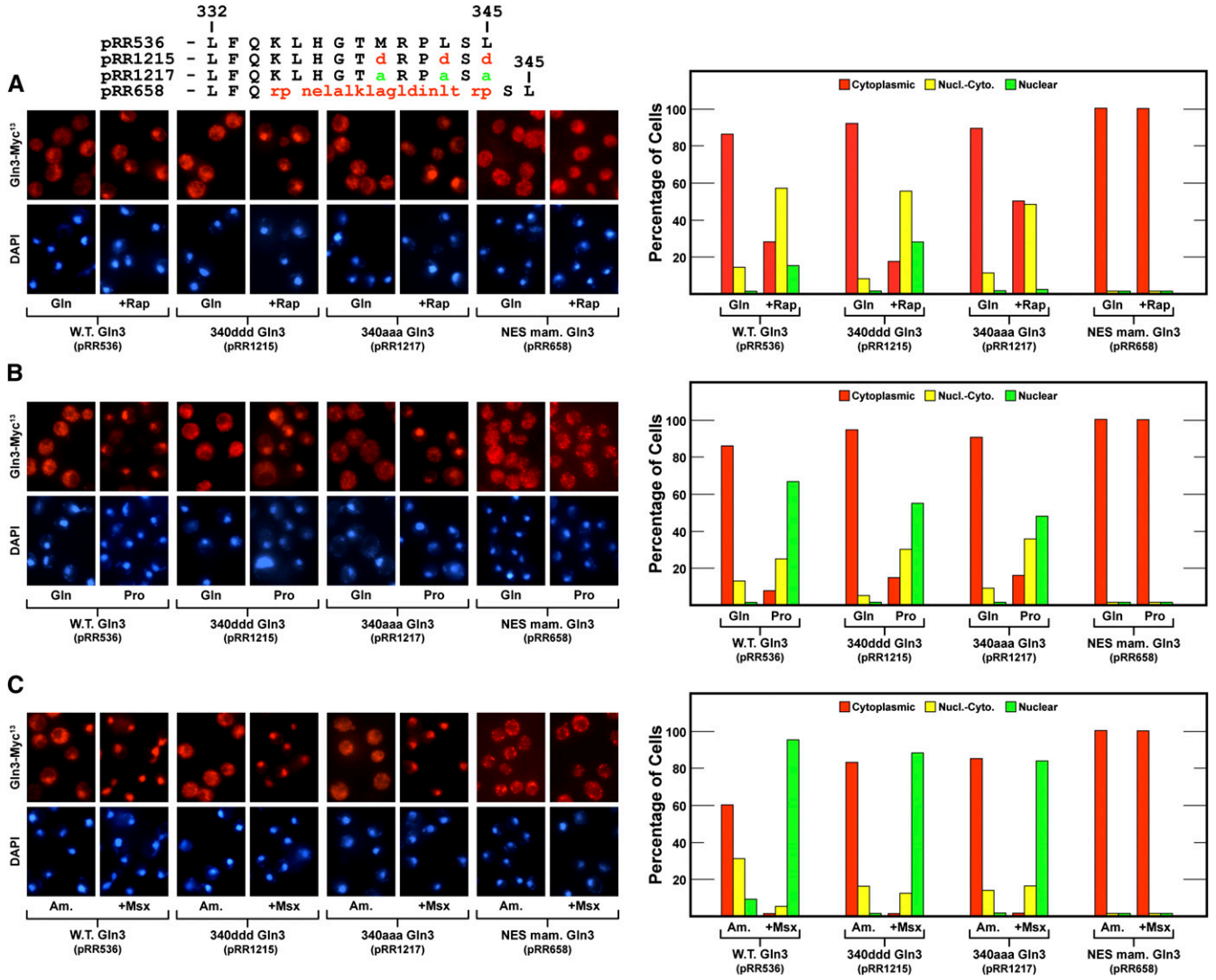

Figure 2 (A–C) Gln3-Myc[13] export was not demonstrably affected by amino acid substitutions in the previously reported Gln3 NESs (pRR1215 and pRR1517) but became constitutive when Gln3 residues 336–345 were replaced with the unregulated mammalian protein kinase inhibitor (PKI) NES (NES mam. Gln3, pRR658). The format of the experiment and data presentation are similar to those described in Figure 1, C–E.

et al. 2004). Three candidate sequences were identified, two with significant confidence as potential NES motifs and a third, the originally reported Gln3$_{336–345}$ sequence. Consistent with our experimental results, the 336–345 sequence rated below the confidence threshold as being a putative NES (Figure 3A). The two newly identified candidates were situated between Gln3 residues 10–20 and 64–73 (Figure 3A). Comparison of these candidate sequences with the canonical NES sequence reported by Carvalho and Zheng (2003) indicated that both were reasonably similar to residues 336–345 (Figure 1A). At the critical four hydrophobic residues, each candidate deviated by the substitution of a bulky hydrophobic amino acid, valine or phenylalanine substituting for the final L345 (Figure 1A, purple letters). It is important to note that in the original analysis demonstrating that Gln3 lacking residues 336–345 failed to interact with Crm1 in a two-hybrid interaction assay, the Gln3 constructs were not full length but rather lacked the N-terminal 141 Gln3 residues and hence Gln3$_{64–73}$ (Carvalho and Zheng 2003).

To evaluate the potential involvement of the new candidate sequences in nuclear Gln3-Myc[13] export, we individually

methionine sulfoximine (E, +Msx) was added where indicated. After incubation (20 and 30 min, respectively), the cultures were again sampled for assay. The intracellular distributions of Gln3-Myc[13] were determined as described in *Materials and Methods*. The precision of Gln3-Myc[13] scoring in the three categories we used is described in *Materials and Methods*. Representative microscopic images of fields from which the histograms were obtained are shown to the left of each set of histograms.

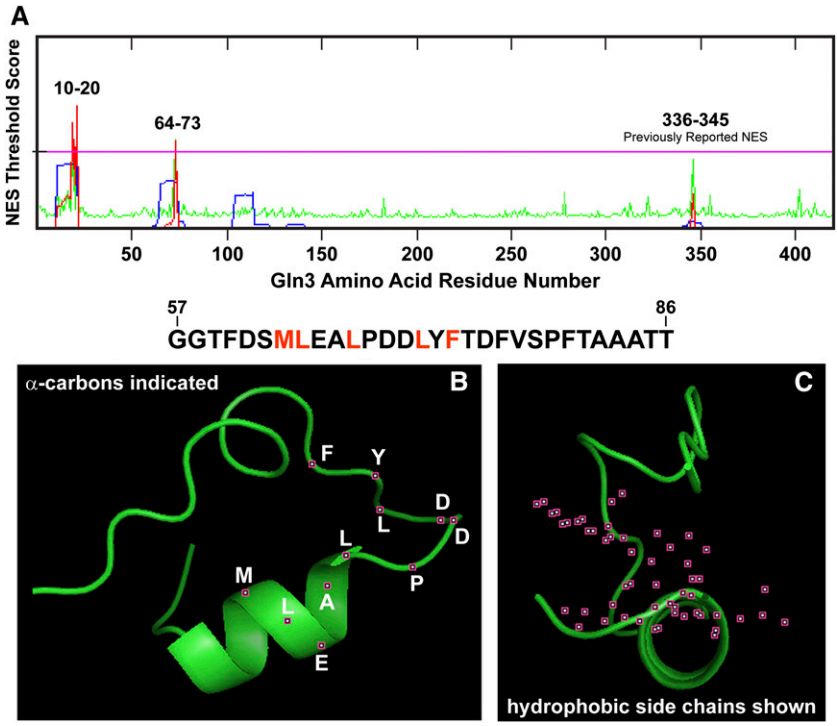

Figure 3 Three Gln3 sequences yielded threshold prediction scores indicating their likelihood of functioning as NES motifs. The computer programs used to generate these outputs are described in the text. (A) The prediction server calculated the overall NES score (red trace) from the hidden Markov model (HMM, blue trace) and artificial neural network (ANN, green trace) scores. If the NES scores of individual residues exceed the threshold value (pink horizontal line), they are predicted to potentially function as a nuclear export signal. (B and C) The predicted most likely structure of Gln3 residues 57–86 (sequence appears above the graphics). Positions of the α-carbon atoms of the residues (white lettering) are indicated in the left image as small maroon boxes with white centers (B). The side-chain atoms of the critical hydrophobic residues in a canonical NES sequence (indicated in red in the sequence above the images) are indicated as small maroon boxes with white centers (C).

deleted them, *gln3*$_{10–20Δ}$-*MYC*^{13} (designated 10–20Δ Gln3, pRR702) and *gln3*$_{64–73Δ}$-*MYC*^{13} (designated 64–73Δ Gln3, pRR714). Even though Gln3 residues 10–20 were predicted with greatest confidence to be homologous to known NESs, deleting them had no demonstrable effect on Gln3-Myc^{13} localization; they behaved the same as wild-type residues (Figure 4). In contrast, 64–73Δ Gln3-Myc^{13} was constitutively nuclear in repressive glutamine- and ammonia-grown cells and derepressive proline-grown cells irrespective of whether or not they were treated with rapamycin or Msx (Figure 5, pRR714).

Sequences participating in nuclear export often begin within an amphipathic α-helix and terminate with an unstructured end so that the terminal hydrophobic LXL residues can interact with other proteins in the export machinery (la Cour *et al.* 2004). Therefore, we modeled the secondary structure of Gln3 residues 57–86 using PEP-FOLD and PHYRE2 and visualized the most likely three-dimensional (3D) structure with PyMOL legacy version 0.99 (Figure 3, B and C). Gln3 residues 63–67 began in the center of a predicted α-helix and extended to an unstructured region beginning with Gln3 proline 68; the locations of the α-carbon atoms of these residues are indicated as small maroon squares with white centers (Figure 3B). Further, the hydrophobic residues in many NESs are situated on one face of the associated α-helix, with the charged residues located on the opposite face. Therefore, we rotated the molecule 90° to the right such that we were looking down the axis of the helix and visualized all side-chain atoms of the hydrophobic residues (red lettering above Figure 3, B and C; in Figure 3C, side-chain atoms are depicted as small maroon boxes with white centers). The hydrophobic residues are clearly situated on one side of the putative α-helix, with neutral and charged residues located on the other side.

Deleting 10 amino acids, four or five of which are hydrophobic, from a protein has the potential of adversely affecting its gross tertiary structure, as well as abolishing the function of the putative motif being investigated. This and the fact that the mutant leading to the original identification of the Gln3 NES was a deletion prompted us to test the preceding results by constructing two additional *gln3* mutants. We substituted aspartate for three of the four critical hydrophobic residues of the putative NES: Gln3$_{L64D,L67R,L71D,F73D}$-Myc^{13} (designated 64drdd Gln3-Myc^{13}, pRR752). The L67R substitution was necessitated by our cloning strategy. The response to these substitutions was the same as occurred when Gln3 residues 64–73 were eliminated by deletion, *i.e.*, constitutively nuclear Gln3-Myc^{13} localization (Figure 6, pRR752).

Alanine and arginine substitutions of the hydrophobic residues, Gln3$_{L64A,L67R,L71A,F73A}$-Myc^{13} (designated 64araa Gln3-Myc^{13}, pRR1090), did not generate nearly as strong a phenotype as the aspartate substitutions, perhaps because alanine is also a hydrophobic amino acid. There was a modest nuclear-cytoplasmic shift of Gln3-Myc^{13} in glutamine-grown rapamycin-treated cells (Figure 6A, pRR1090) and decreased cytoplasmic localization in ammonia-grown cells (Figure 6C, pRR1090). Together these data supported the contention that Gln3 residues 64–73 were required for nuclear Gln3 export when cells were cultivated in repressive nitrogen-rich medium. Further, the fact that 64drdd Gln3-Myc^{13} (pRR752) was constitutively nuclear was consistent with the idea that

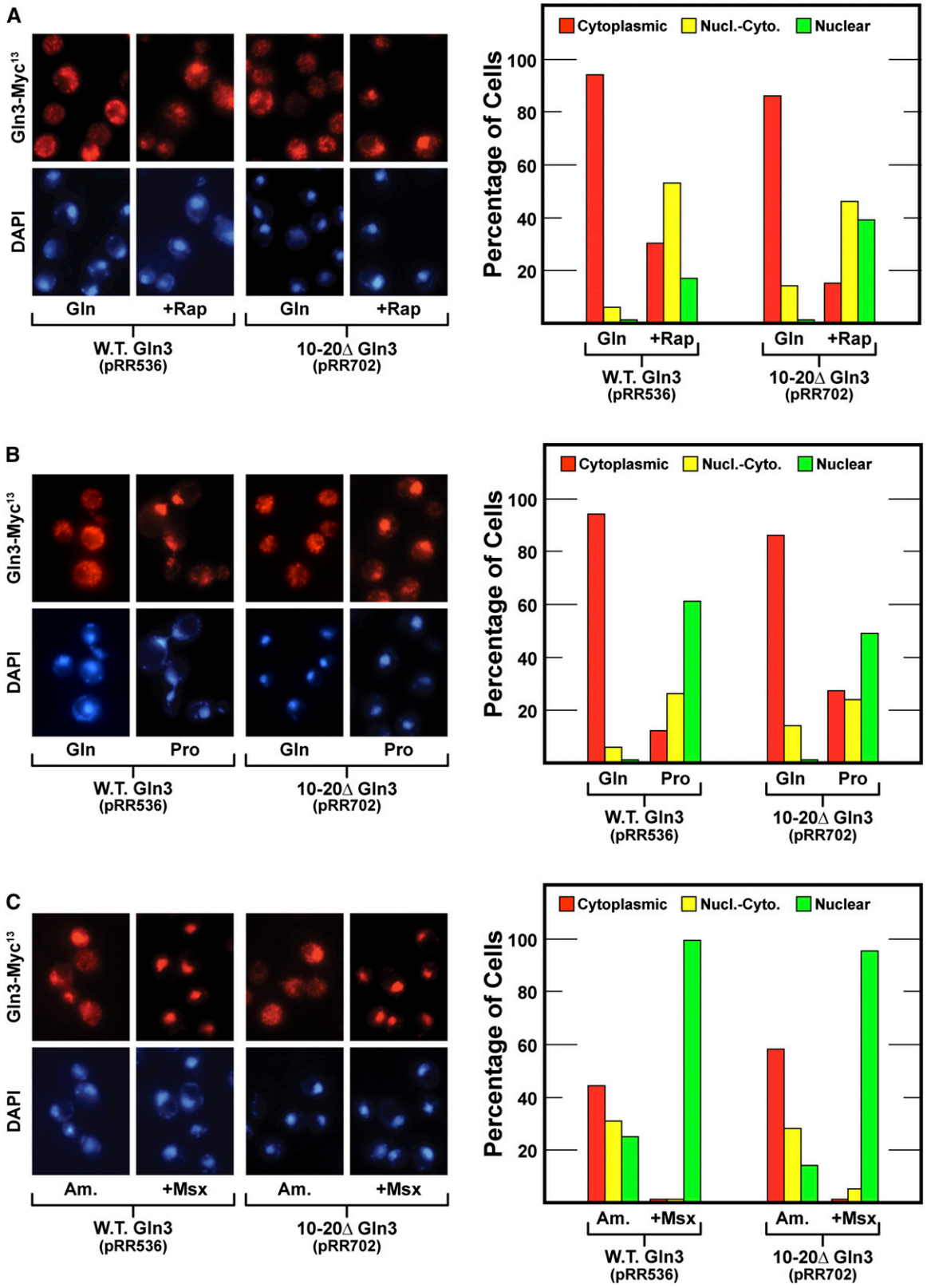

Figure 4 (A–C) Deletion of Gln3 residues 10–20 (pRR702) with the highest probability of being a NES signal does not demonstrably affect Gln3-Myc^{13} intracellular localization. The format of the experiment and data presentation are similar to those described in Figure 1, C–E.

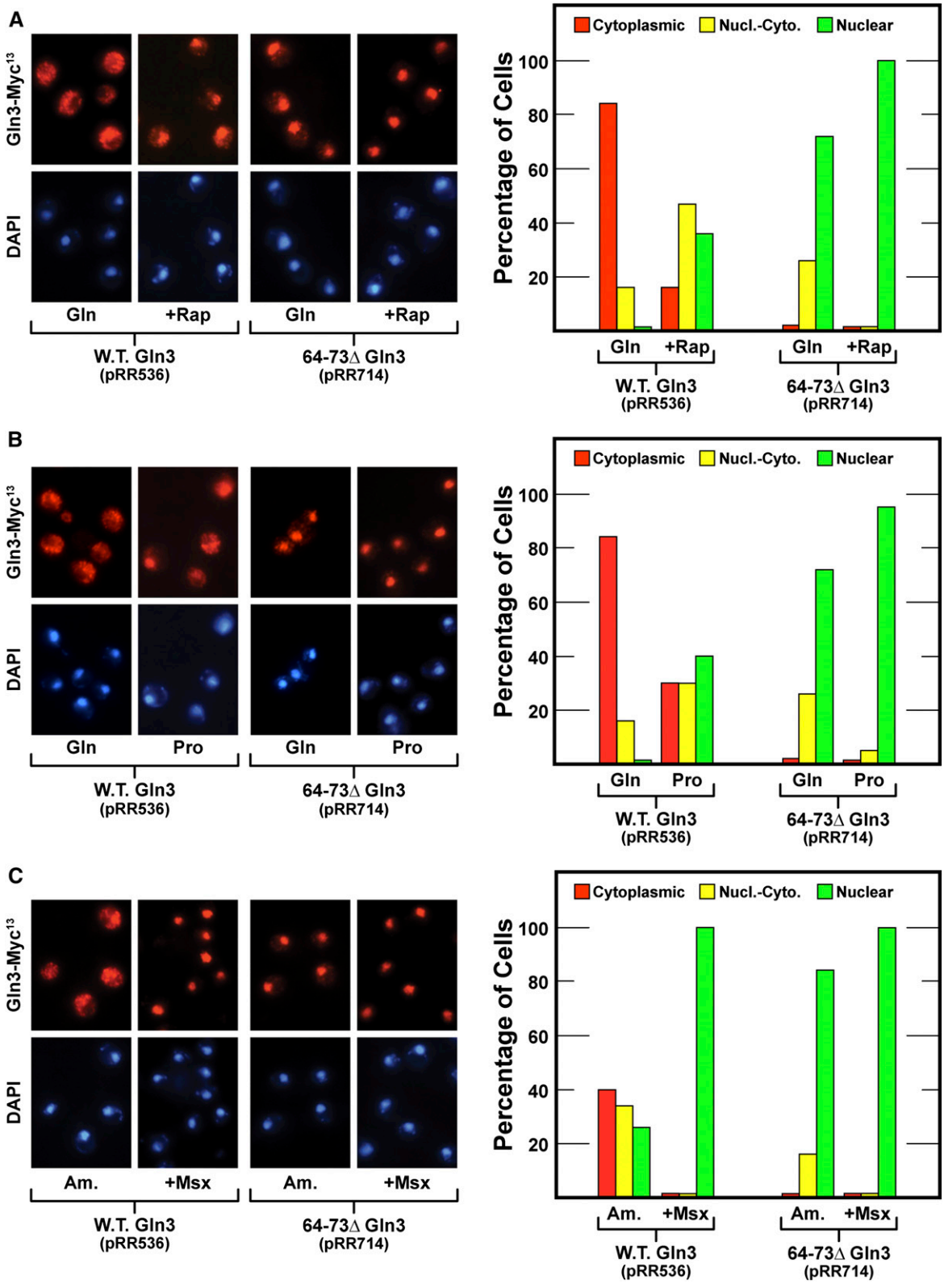

Figure 5 (A–C) Gln3-Myc^{13} export is abolished, thus sequestering Gln3 within the nucleus of cells lacking Gln3 residues 64–73 (pRR714). The format of the experiment and data presentation are similar to those described in Figure 1, C–E.

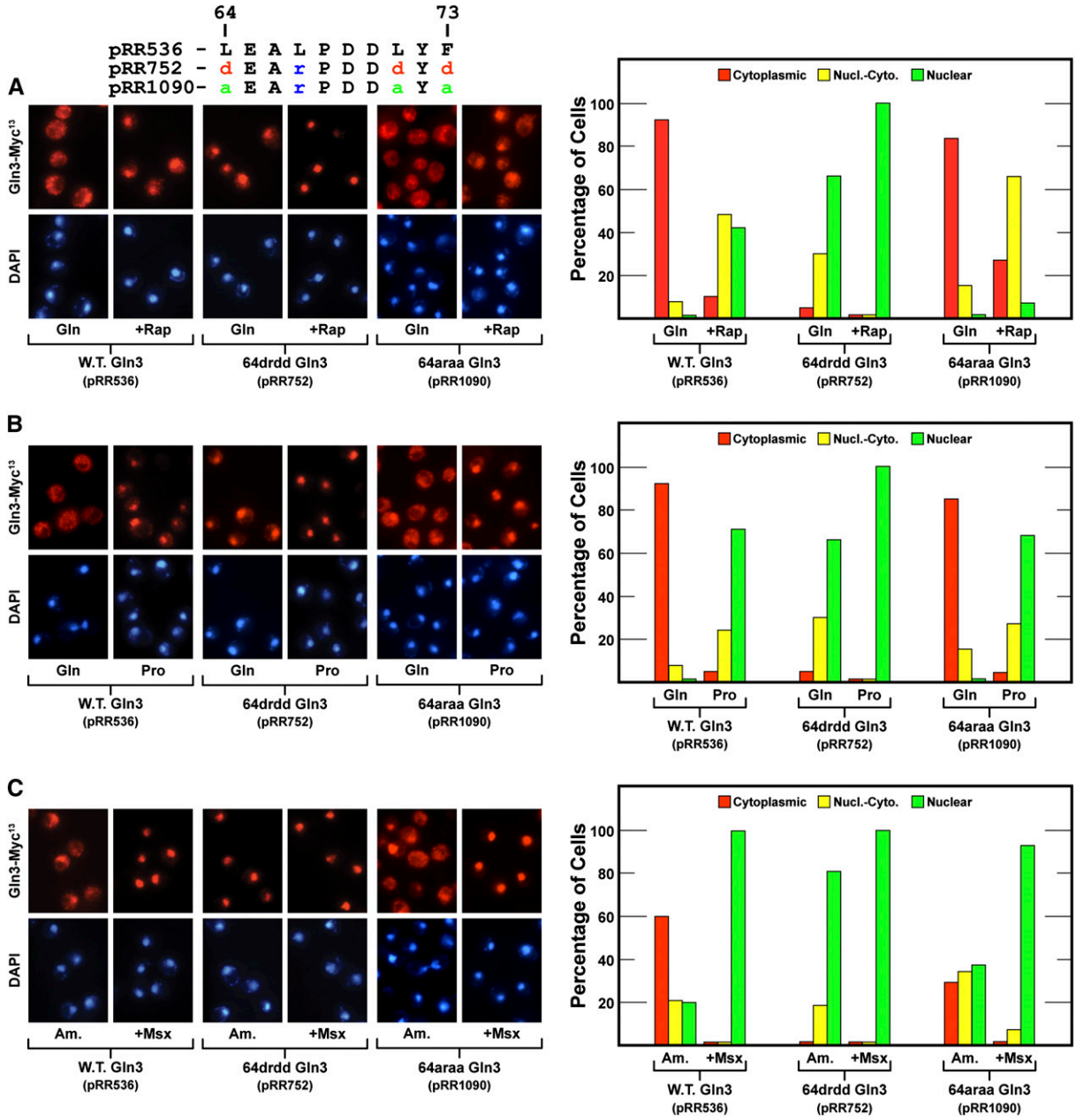

Figure 6 (A–C) Gln3-Myc^{13} localization in mutants containing substitutions of the hydrophobic residues in Gln3$_{64–73}$. The mutants assayed were Gln3$_{L64D,L67R,L71D,F73D}$-Myc^{13} (pRR752) and Gln3$_{L64A,L67R,L71A,F73A}$-Myc^{13} (pRR1090). The format of the experiment and data presentation are similar to those described in Figure 1, C–E.

residues 64–73 were the only demonstrably functioning Gln3 NES under the culture conditions we assayed.

Did alteration of Gln3$_{64–73}$ or Gln3$_{332–345}$ abolish nuclear Gln3-Myc^{13} export or Gln3-Myc^{13}–Ure2 interaction?

There was, however, an alternative interpretation of the preceding data that merited equal consideration. The phenotype of a NES mutant is constitutively nuclear Gln3, which is also the phenotype of *ure2*Δ mutants. Ure2 is required to sequester Gln3 in the cytoplasm and restrict NCR-sensitive transcription to basal levels in nitrogen-replete repressive conditions (Drillien and Lacroute 1972; Drillien *et al.* 1973; Courchesne and Magasanik 1988; Blinder *et al.* 1996; Bertram *et al.* 2000; Kulkarni *et al.* 2001; Carvalho and Zheng 2003; Feller *et al.* 2013). Since the Ure2 binding domain in Gln3 is situated between Gln3 residues 102 and 150 (Kulkarni *et al.* 2001; Carvalho and Zheng 2003), we were concerned that alterations in the Gln3$_{64–73}$ (pRR752) or Gln3$_{332–345}$ (pRR787 and pRR1215) regions might have adversely affected Gln3-Ure2 complex formation. An earlier observation that Gln3 lacking its 101 N-terminal residues yielded reduced co-immunoprecipitation of Ure2 was consistent

with this concern (Carvalho and Zheng 2003). However, Carvalho and Zheng (2003) also demonstrated that Gln3 residues 102–150 were alone sufficient to yield a wild-type Gln3-Ure2 interaction.

Therefore, it was necessary to address two questions: (1) did Gln3 containing alterations of residues in $Gln3_{64–73}$ (64drdd Gln3-Myc^{13}, pRR752) or in $Gln3_{332–345}$ (332dddd Gln3-Myc^{13}, pRR787, and 340ddd Gln3-Myc^{13}, pRR1215) continue to interact with Ure2, or (2) if 64drdd Gln3-Myc^{13} did interact with Ure2, could we explain why reduced Gln3-Ure2 co-immunoprecipitation was observed when the N-terminal Gln3 residues 1–101 were abolished? Our first approach to these questions was to compare the phenotypes exhibited by wild-type (pRR536) and mutant (pRR787, pRR1215, and pRR752) plasmids when asparagine- or glutamine-grown wild-type and *ure2*Δ strains were used as the transformation recipients. In short, was Ure2 functioning to maintain Gln3-Myc^{13} in the cytoplasm of cells cultured in nitrogen-replete conditions? Gln3-Myc^{13} was almost completely cytoplasmic in glutamine-grown wild-type cells containing pRR536, pRR787, and pRR1215, whereas in the *ure2*Δ mutant it became nuclear (Figure 7A). The same results were observed when pRR536 and pRR1215 were transformed into asparagine-grown cells. However, because Gln3-Myc^{13} was already nuclear in asparagine-grown wild-type cells containing pRR787, deleting *URE2* had little effect (this observation will be explained later). In the case of pRR752, 64drdd Gln3-Myc^{13} was nuclear in about two-thirds of the asparagine-grown wild-type cells and nuclear-cytoplasmic or cytoplasmic in about a third (Figure 7A). If Ure2 were able to function with 64drdd Gln3-Myc^{13}, then deleting *URE2* should result in 64drdd Gln3-Myc^{13} becoming more nuclear. This was observed experimentally: 64drdd Gln3-Myc^{13} became completely nuclear in both asparagine- and glutamine-grown *ure2*Δ cells (Figure 7A). Together these results indicated that Ure2 functioned normally when residues in the $Gln3_{332–345}$ and $Gln3_{64–73}$ regions were altered, although the demonstration could not be as dramatic with pRR752 because 64drdd Gln3-Myc^{13} was already significantly nuclear in the wild-type transformation recipient.

Given the modest *ure2*Δ effect with 64drdd Gln3-Myc^{13} (pRR752) localization, we asked whether Ure2 could be co-immunoprecipitated with wild-type (pRR536) and mutant (pRR787 and pRR752) forms of Gln3-Myc^{13}. This was a conceptually more complex challenge because Ure2 is cytoplasmic, whereas Gln3-Myc^{13} is largely nuclear in pRR787 and pRR752 transformants. To circumvent this problem, we transformed asparagine-grown wild-type cells (TB50) with two plasmids, the Gln3-Myc^{13} plasmid to be analyzed (pRR536, pRR752, or pRR787) and pAA15, which carried a NLS-LexA-Ure2 fusion (Kulkarni *et al.* 2001). The NLS-LexA-Ure2 fusion protein was shown previously to bind Gln3, which retained its ability to mediate NCR-sensitive transcription even though bound to NLS-LexA-Ure2 (Kulkarni *et al.* 2001). Before employing this new approach, we assessed the effectiveness and specificity of the individual antibodies against Myc and LexA in immunoprecipitating these proteins from crude extracts. Western blot analyses of cultures containing only Gln3-Myc^{13} (pRR536) or NLS-LexA-Ure2 (pAA15) demonstrated that the two individual antibodies were very specific and did not exhibit any cross-reaction (Figure 7D). In the case of Gln3-Myc^{13}, 30 min of incubation with the immunobeads was not as effective as 2 hr (Figure 7B, lanes 1 and 3 *vs.* lanes 4 and 6). For NLS-LexA-Ure2, there was no great difference between the two incubation times (Figure 7C, lanes 1 and 3 *vs.* lanes 4 and 6). However, in both cases, substantially more and more extensive degradation of the ligands occurred following binding to the immunobeads than in crude extracts. Note the most rapidly migrating Gln3-Myc^{13} species and a second more rapidly migrating NLS-LexA-Ure2 species (arrow) in Figure 7, B and C (lanes 3 and 4). These data indicated that the co-immunoprecipitation assays were functioning properly but that degradation, especially of Gln3-Myc^{13}, could be anticipated.

To co-immunoprecipitate NLS-LexA-Ure2 with Gln3-Myc^{13}, we prepared extracts from asparagine-grown transformants containing NLS-LexA-Ure2 (pAA15) along with wild-type Gln3 (pRR536) or Gln3 mutants (pRR752 or pRR787) (Figure 7F, lanes 1–3). These extracts were incubated with anti-Myc immunobeads, and the bound proteins were recovered and subjected to parallel Western blot analyses probed with either anti-Myc or anti-LexA antibodies (Figure 7D, top, middle, and bottom blots, respectively, lanes 4–6). There were clear though substantially reduced immunoprecipitated full-length Gln3-Myc^{13} species in the wild-type, pRR536, and pRR787 lanes (Figure 7F, top blot, lanes 4 and 5) but not in the pRR752 lane (lane 6). The Gln3-Myc^{13} degradation product, however, was present in lanes 4–6. Gross overexposure of the upper blot in Figure 7F clearly showed the lack of signal in lane 6, diminished signals in lanes 4 and 5, and the crude extract in lane 1 derived from the fact that heavy degradation had occurred during the analysis (Figure 7F, overexposed bottom blot). Rather remarkably, however, despite Gln3-Myc^{13} degradation, there were strong NLS-LexA-Ure2 signals with all three plasmids when a parallel blot was probed with anti-LexA antibody (Figure 7F, middle blot, lanes 4–6). A faster migrating Ure2 degradation product also was present (fastest migrating species in lanes 4–6). These data indicated that Ure2 was able to bind to all three Gln3 proteins and further suggested that the Gln3-Myc^{13}–NLS-LexA-Ure2 complex was more stable than Gln3-Myc^{13} alone, an observation reported previously (Bertram *et al.*, 2000; Carvalho and Zheng 2003). We next repeated the transformation, but this time using glutamine-grown cells so that the effects of both nitrogen sources were analyzed. Extracts of these cultures were incubated with anti-LexA immunobeads, and bound proteins were recovered and subjected to parallel Western blots, as described earlier. As we predicted from the preceding experiments, the Gln3-Myc^{13}–NLS-LexA-Ure2 complex was much more stable than Gln3-Myc^{13} alone. As a result, our recoveries of full-length Gln3-Myc^{13} bound to the anti-LexA immunobeads were much better and had less Gln3 degradation (Figure 7G, top blot). These results clearly

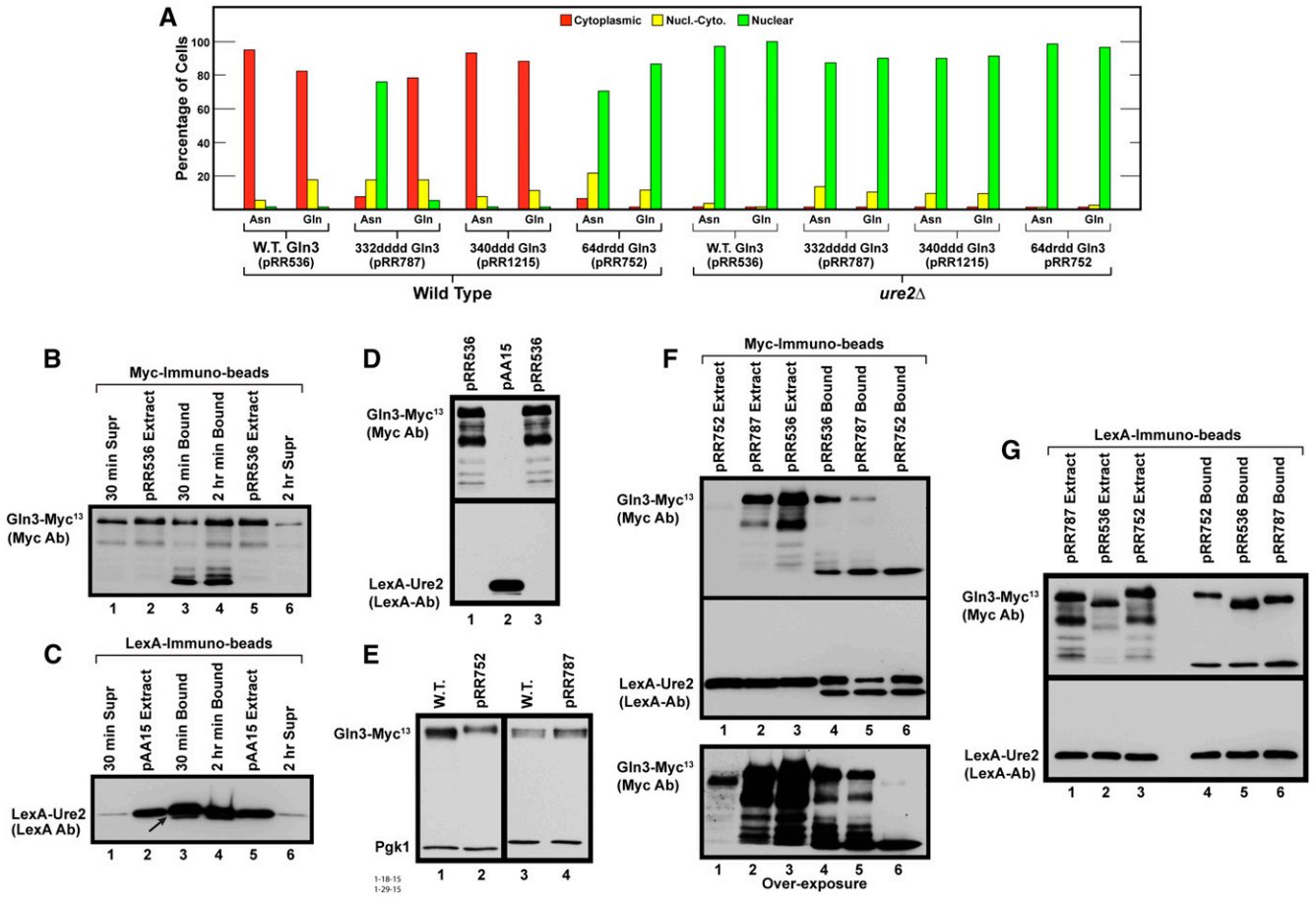

Figure 7 Ure2 binds to and functions with mutant forms of Gln3-Myc^{13}. (A) The effects of deleting *URE2* on glutamine- or asparagine-grown wild-type and mutant Gln3$_{L332D,L336D,M340D,L343D}$-Myc^{13} (pRR787), Gln3$_{M340D,L343D,L345D}$-Myc^{13} (pRR1215), or Gln3$_{L64D,L67R,L71D,F73D}$-Myc^{13} (pRR752) localization. Wild-type (pRR536) or mutant (pRR787, pRR1215, and pRR752) plasmids were transformed into wild-type (JK9-3da) or *ure2*Δ (RR215) strains. These transformants were assayed and the data presented as described in Figure 1, C–E. (B and C) Time-dependent binding of wild-type (pRR536) Gln3-Myc^{13} and NLS-LexA-Ure2 to anti-Myc and anti-LexA immunobeads. An extract of TB50 transformed with both pRR536 and pAA15 was bound to anti-Myc or anti-LexA immunobeads, respectively, for either 30 min or 2 hr at 4°. Supernatants (Supr) remaining after proteins in the extracts were bound to the immunobeads and proteins eluted from the immunobeads (Bound) and extracts from wild-type (pRR536) or NLS-LexA-Ure2 (pAA15) cultures were subjected to Western blot analyses. The blots were probed with either anti-Myc (B) or anti-LexA (C) antibodies. (D) Anti-Myc and anti-LexA antibodies are highly specific, exhibiting no cross-reaction. Extracts were prepared from glutamine-grown transformants containing either wild-type Gln3-Myc^{13} (pR536) or NLS-LexA-Ure2 (pAA15), as described in *Materials and Methods*. These extracts were then loaded into parallel gels, and the blots emanating from them were probed with anti-Myc (top blot) or anti-LexA antibodies (bottom blot). (E) Wild-type Gln3-Myc^{13} (pRR536), Gln3$_{L64D,L67R,L71D,F73D}$-Myc^{13} (pRR752), and Gln3$_{L332D,L336D,M340D,L343D}$-Myc^{13} (pRR787) proteins are present in similar amounts *in vivo*. Extracts from either wild-type (pRR536) or mutant (pRR752 and pRR787) Gln3-Myc^{13} YNB-asparagine-grown cultures were precipitated with trichloroacetic acid and subjected to SDS-PAGE, and the blots were simultaneously probed with anti-Myc and anti-Pgk1 antibodies. Pgk1 was used to assess gel loading and transfer. Compare them with the behavior of extracts analyzed in B, F, and G. (F) NLS-LexA-Ure2 immunoprecipitates with Gln3-Myc^{13}. Extracts were prepared from an asparagine-grown wild-type recipient TB50 transformed with pAA15 (NLS-LexA-Ure2) and either pRR536 (wild-type Gln3-Myc^{13}), pRR787 (Gln3$_{L332D,L336D,M340D,L343D}$-Myc^{13}), or pRR752 (Gln3$_{L64D,L67R,L71D,F73D}$-Myc^{13}). The extracts were bound to anti-Myc immunobeads for 30 min at 4° to immunoprecipitate Gln3-Myc^{13} and proteins potentially bound to it. Extracts and proteins eluted from the anti-Myc immunobeads then were subjected to two parallel Western blot analyses. One of the blots was probed with anti-Myc antibodies (top and bottom blots) and the other with anti-LexA antibodies (middle blot). The blot probed with anti-Myc antibodies (top blot) was vastly overexposed (bottom blot) to visualize the degraded Gln3-Myc^{13} proteins it contained. (G) Gln3-Myc^{13} immunoprecipitates with NLS-LexA-Ure2. Extracts were prepared from a glutamine-grown wild-type recipient TB50 transformed with pAA15 (NLS-LexA-Ure2) and pRR536 (wild-type Gln3-Myc^{13}), pRR787 (Gln3$_{L332D,L336D,M340D,L343D}$-Myc^{13}), or pRR752 (Gln3$_{L64D,L67R,L71D,F73D}$-Myc^{13}). The extracts were bound to anti-LexA immunobeads for 15 min at 4° to immunoprecipitate NLS-LexA-Ure2 and proteins potentially bound to it. Extracts and proteins eluted from the anti-LexA immunobeads then were subjected to two parallel Western blot analyses. One of the blots then was probed with anti-Myc antibodies (top blot) and the other with anti-LexA antibodies (bottom blot).

indicated that Gln3-Myc^{13} and NLS-LexA-Ure2 coprecipitated irrespective of the immunoabsorbent used.

The observed *in vitro* lability of Gln3-Myc^{13} derived from pRR787 and pRR752 raised the possibility that it might be as labile *in vivo* as *in vitro*, even though the intracellular localization data observed with these plasmids did not favor this possibility. Therefore, we posed the question more directly by breaking cells in trichloroacetic acid, which minimizes

proteolysis, rather than in the co-immunoprecipitated lysis buffer designed to maintain *in vivo* binding functions. We compared Western blots of wild-type Gln3-Myc^{13} (pRR536), 332dddd Gln3-Myc^{13} (pRR787), and 64drdd Gln3-Myc^{13} (pRR752) in asparagine-grown transformants. The wild-type and mutant levels of Gln3-Myc^{13} were similar (Figure 7E). These data indicated that the gross degradation of both wild-type and mutant proteins observed in the co-immunoprecipitated blots derived from *in vitro* Gln3-Myc^{13} lability in the co-immunoprecipitated conditions employed rather than *in vivo* instability.

Together these approaches demonstrated that Ure2 retained its ability to bind to both 64drdd Gln3-Myc^{13} (pRR752) and 332dddd Gln3-Myc^{13} (pRR787). Further, Ure2 functioned normally to sequester 332dddd Gln3-Myc^{13} and 340ddd Gln3-Myc^{13} (pRR1215) in the cytoplasm of cells provided with a repressive nitrogen source. Ure2 also appeared to function normally with 64drdd Gln3-Myc^{13} in that its cytoplasmic sequestration decreased in the *ure2*Δ mutants; the effect was modest, however, because 64drdd Gln3-Myc^{13} was already so nuclear in the wild-type Gln3-Myc^{13}. Therefore, it was unlikely that the nuclear localization of these mutant Gln3s derived from altered secondary structures that adversely affected Ure2 binding or function. The data also explained why the previously analyzed 1–101 N-terminal Gln3 truncation yielded reduced Ure2-Gln3-Myc^{9} co-immunoprecipitation. While the previously reported extracts possessed similar amounts of protein (Carvalho and Zheng 2003), once bound to the immunobeads, the truncated Gln3-Myc^{9}, being more labile than wild-type Gln3-Myc^{9} *in vitro*, yielded a reduced signal.

Previously reported Gln3 NES deletion abolishes the DNA binding site

Our next objective was to rectify the paradoxical phenotypes of the *gln3*Δ that Carvalho and Zheng (2003) originally characterized and the mutant we isolated, pRR787. Why did Gln3 constitutively localize to the nucleus when residues 336–345 were abolished but did not behave similarly in the three substitution mutants we constructed, in particular, 332dddd Gln3-Myc^{13} (pRR787)? To address this question, we looked in detail at the amino acid sequence around Gln3 residues 336–345 and discovered that they were immediately adjacent to the Gln3 zinc finger motif responsible for Gln3 binding to its target GATA elements in NCR-sensitive gene promoters (Cooper *et al.* 1989; Rai *et al.* 1989; Bysani *et al.* 1991; Blinder and Magasanik 1995; Cunningham *et al.* 1996; Stanbrough and Magasanik 1996). This entire region of Gln3, residues 306–357, is highly conserved in both closely and more distantly related yeasts (Figure 8A). Equally important, high sequence identity exists between the *S. cerevisiae* Gln3 and *Aspergillus nidulans* AREA DNA binding domains (Figure 8A). Sequence identity is also observed to a more limited extent with the human hGATA-1 and hGATA-2 and chicken cGATA-1 proteins (Figure 8A). Like Gln3, the AREA and cGATA-1 proteins are GATA-binding proteins (Orkin 1992; Merika and Orkin 1993; Ko and Engel 1993; Ravagnani *et al.* 1997; Scazzocchio 2000). To our advantage, 3D structures of AREA and cGATA-1 in complexes with their GATA DNA target sites have been determined using NMR methods (Merika and Orkin 1993; Omichinski *et al.* 1993a,b; Stahl and Gronenborn 1993; Starich *et al.* 1998; Kotaka *et al.* 2008; Scazzocchio 2000).

AREA and cGATA-1 zinc fingers consist of two β-sheets that form a coordination complex with a zinc ion followed by an α-helix and an unstructured loop (Figure 8C, image A). The α-helix contacts nucleotides in the major groove of the DNA while the unstructured loop folds around to interact with nucleotides in the adjacent minor groove. AREA residues contacting the DNA are indicated by small black boxes at the top of the homology series (Figure 8A) and as yellow portions of the AREA 3D ribbon structure (Figure 8C, image A). Bases of the DNA-contacting AREA amino acids are also indicated as yellow portions of the blue and maroon DNA strands in Figure 8C (images A–D).

The near identity of the Gln3 and AREA DNA-contacting residues and the fact that the 3D structure of the AREA-DNA complex was available permitted us to assess the relation between the Gln3 DNA binding domain and the 336–345 deletion that generated nuclear Gln3 localization. This deletion eliminated four amino acids predicted to contact the DNA GATA sequence (Figure 8, A and B, long red box). The abolished amino acids, 336–345, are indicated as the yellow portion of the Gln3 3D ribbon structure in Figure 8C (image B). Equally important, loss of residues 336–345 drastically alters the alignment of the unstructured loop that would normally lie in the adjacent minor groove by advancing it to the end of the α-helix (Figure 8C, image B, dashed white arrow). As a result, nine rather than four Gln3 DNA contacts are lost in the deletion. The Gln3 DNA binding domain is virtually destroyed by the 336–345 deletion. The DNA binding domain in 332dddd Gln3 (pRR787) also was likely to be heavily damaged because of the locations where we substituted charged amino acids for hydrophobic ones (Figure 8C, image C, yellow portions of the 3D ribbon structure). In contrast, substitutions in 340ddd Gln3 (pRR1215) occurred in the loop situated between the major and minor grooves that do not contact the DNA (Figure 8C, image D, yellow portions of the 3D ribbon structure).

These observations and reasoning generated a testable series of predictions extending from Gln3-dependent growth to Gln3-mediated transcription and DNA binding. Loss of Gln3 NES function would be expected to adversely affect regulated Gln3 localization but not its ability to activate transcription and hence support Gln3-dependent growth. In contrast, loss or significant damage of the Gln3 DNA binding domain would be expected to adversely affect Gln3-dependent transcription and with it Gln3-dependent growth. These expectations were based on the phenotypes of a broad array of amino acid substitutions in the *A. nidulans* AREA GATA-binding domain that result in loss of ability to grow on nitrogen sources that require NCR-sensitive gene products (Arst and Cove 1973; Hynes

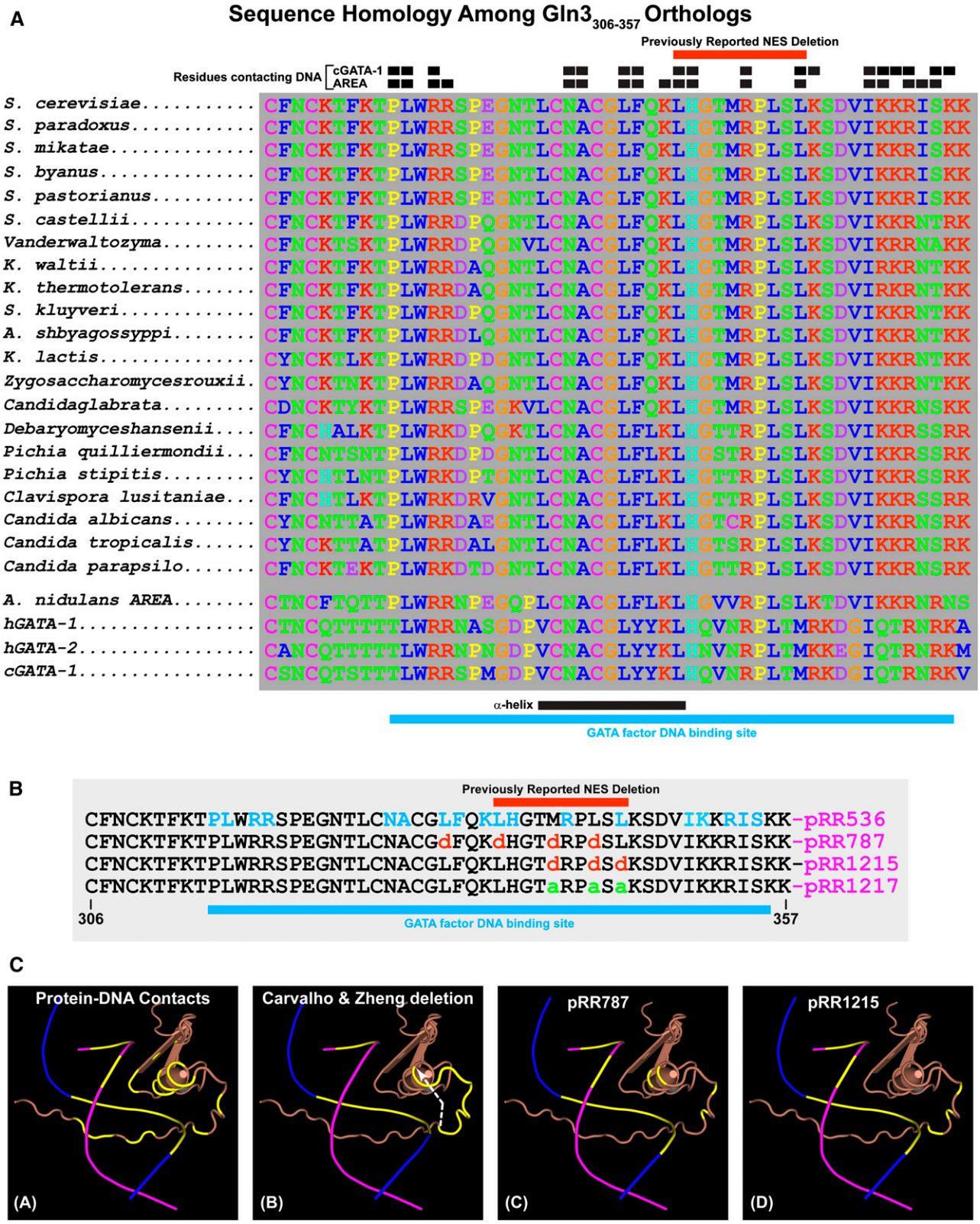

Figure 8 (A) Sequence homologies among $Gln3_{306–357}$ orthologs. Black boxes above the homologous sequences indicate residues of the cGATA-1 and AREA GATA factor binding proteins that contact their target DNA sequences. Red bars above the homologous sequences indicate the residues eliminated in the deletion described by Carvalho and Zheng (2003). Black and blue bars beneath the homologous sequences indicate the positions of the α-helix portion of the zinc finger motif and GATA factor DNA binding site, respectively. (B) Amino acid substitutions in the Gln3 wild-type sequence (pRR536) and the plasmids that contain them. Residues that contact the AREA/Gln3 DNA binding site are indicated in blue letters (pRR536).

1975; Kudla *et al.* 1990; Langdon *et al.* 1995; Platt *et al.* 1996a,b). We compared growth of wild-type (pRR536), 340ddd Gln3-Myc^{13} (pRR1215), 64araa Gln3-Myc^{13} (pRR1090), 64drdd Gln3-Myc^{13} (pRR752), and 332dddd Gln3-Myc^{13} (pRR787) transformants in both repressive (glutamine) and derepressive (proline or allantoin) media (Figure 9A). Proline and allantoin are poor nitrogen sources whose degradation is Gln3 dependent. Since Gln3 and Gat1 partially share transcriptional activation functions, a *gln3*-Δ*gat1*Δ mutant was used as the transformation recipient so that growth would be solely dependent on active Gln3. Growth of 340ddd Gln3-Myc^{13} (pRR1215), 64araa Gln3-Myc^{13} (pRR1090), and 64drdd Gln3-Myc^{13} (pRR752) transformants was the same as wild type (pRR536) when glutamine, proline, or allantoin was provided as the sole nitrogen source (Figure 9A, images A–L). In contrast, the 332dddd Gln3-Myc^{13} (pRR787) and vector (pRS316) transformants grew normally in glutamine medium but only minimally in proline or allantoin medium (Figure 9A, images M–O), thus fulfilling the expected growth characteristics of mutants with defects in a Gln3 NES and zinc finger DNA binding motif, respectively.

We next assessed the substitution mutants' predicted rapamycin sensitivities, which also depend on Gln3-mediated transcription. First, *gln3* substitution mutants lacking NES function accumulate Gln3 in the nucleus and hence should exhibit rapamycin hypersensitivity. This phenotype should *a priori* be similar to the one reported for a *ure2*Δ mutation, which also results in constitutively nuclear Gln3 and Gat1 localization (Bertram *et al.* 2000; Carvalho and Zheng 2003; Feller *et al.* 2013, Tate *et al.* 2015). Second, in contrast, *gln3* substitution mutants with a damaged DNA binding domain should be unable to effectively activate NCR-sensitive transcription and hence should exhibit rapamycin resistance, a phenotype similar to that of a *gln3*Δ mutant (Beck and Hall 1999; Bertram *et al.* 2000; Carvalho and Zheng 2003). Transformants (*gln3*Δ, *gat1*Δ recipient) containing plasmid-borne *gln3* alleles with substitutions in the putative NES [64drdd Gln3-Myc^{13} (pRR752) and 64araa Gln3-Myc^{13} (pRR1090)] were just barely more sensitive than wild-type Gln3 (pRR536) (Figure 9B). This was less rapamycin sensitivity than expected or would be observed if a *ure2*Δ but otherwise wild-type strain were assayed. The less than expected hypersensitivity occurred because two functional GATA transcription activators (Gln3 and Gat1) cumulatively contribute to the *ure2*Δ mutant phenotype, whereas transformants of pRR752 and pRR1090 contained only one activator (Gln3-Myc^{13}). In sharp contrast, substitutions in residues contacting the DNA [332dddd Gln3-Myc^{13} (pRR787) and 340ddd Gln3-Myc^{13} (pRR1215)] resulted in transformants that were highly rapamycin resistant, as predicted (Figure 9B).

These results cumulatively suggested that 332dddd Gln3-Myc^{13}–mediated transcription was significantly damaged. Therefore, we directly determined whether or not this was the case by measuring expression of the NCR-sensitive *GDH2* gene using qualitative RT-PCR. As predicted, 332dddd Gln3-Myc^{13} supported only about one-quarter of the NCR-sensitive *GDH2* (NAD-glutamic dehydrogenase) transcription as wild-type Gln3-Myc^{13} (Figure 9D). Finally, we determined whether the inability of 332dddd Gln3-Myc^{13} (pRR787) to mediate NCR-sensitive transcription correlated directly with loss of its ability to bind GATA DNA in an EMSA. We employed the highly characterized oligonucleotide from the NCR-sensitive *DAL3* (allantoate permease) promoter, originally used to establish Gln3 binding to GATA sequences, as the probe (Cunningham *et al.* 1996). An extract derived from a wild-type pRR536 transformant yielded a high-molecular-weight complex with this target DNA, indicative of DNA binding (Figure 9C, right panel, lanes 1, 3, and 6), whereas extracts from transformants of pRR787 or control vector (pRS316), as well as the minus protein control, did not (Figure 9C, right panel, lanes 2, 4, and 5, respectively). Given the sensitivity of Gln3 to proteolysis *in vitro*, Western blots were used to verify that the amounts of protein extract loaded into lanes of the EMSA gel were similar and similarly intact (Figure 9C, left panel). Although there was slightly more *in vitro* proteolysis of the 332dddd Gln3-Myc^{13} compared to wild type, both proteins were largely intact and present in similar amounts in the EMSAs. These data were cumulatively consistent with the contention that deletion of residues 336–345 or alterations in DNA-contacting residues [332dddd Gln3-Myc^{13} (pRR787) and 340ddd Gln3-Myc^{13} (pRR1215)] severely damaged Gln3-Myc^{13} binding to its GATA target sites in NCR-sensitive promoters.

Intracellular localization of 332dddd Gln3-Myc^{13} is strongly influenced by the medium complexity

Although the preceding reasoning and experiments supported the conclusions that the Gln3 NES consisted of residues 64–73 rather than 336–345 and that alteration of residues 332–345 severely impaired Gln3-Myc^{13} DNA binding, they failed to explain why their elimination resulted in constitutive nuclear localization of Gln3-Myc^{9}, as reported previously (Carvalho and Zheng 2003). Revisiting that earlier work, we noticed that the experiments were performed in complex SC medium containing both ammonia and amino acids, whereas minimal YNB medium containing single nitrogen sources was used in our experiments.

Blue bar beneath the sequences indicates the overall DNA binding site. (C) Three-dimensional renderings of the AREA and, by analogy, Gln3 zinc finger DNA complex. DNA strands appear as blue and maroon lines, with the bases that contact AREA/Gln3 protein indicated in yellow. The AREA/Gln3 protein residues appear in brown. (Image A) Contact residues and bases of AREA/Gln3 protein and DNA are indicated in yellow. (Image B) Bases of the DNA in contact with AREA/Gln3 are indicated in yellow. AREA/Gln3 residues eliminated in the Carvalho and Zheng (2003) deletion are also indicated in yellow. A white arrow indicates the shift in the zinc finger motif's coiled coil as a result of eliminating the intervening residues, thereby abolishing their interactions with normal DNA contacts. (Images C and D) Residues substituted in pRR787 and pRR1215 are indicated in yellow.

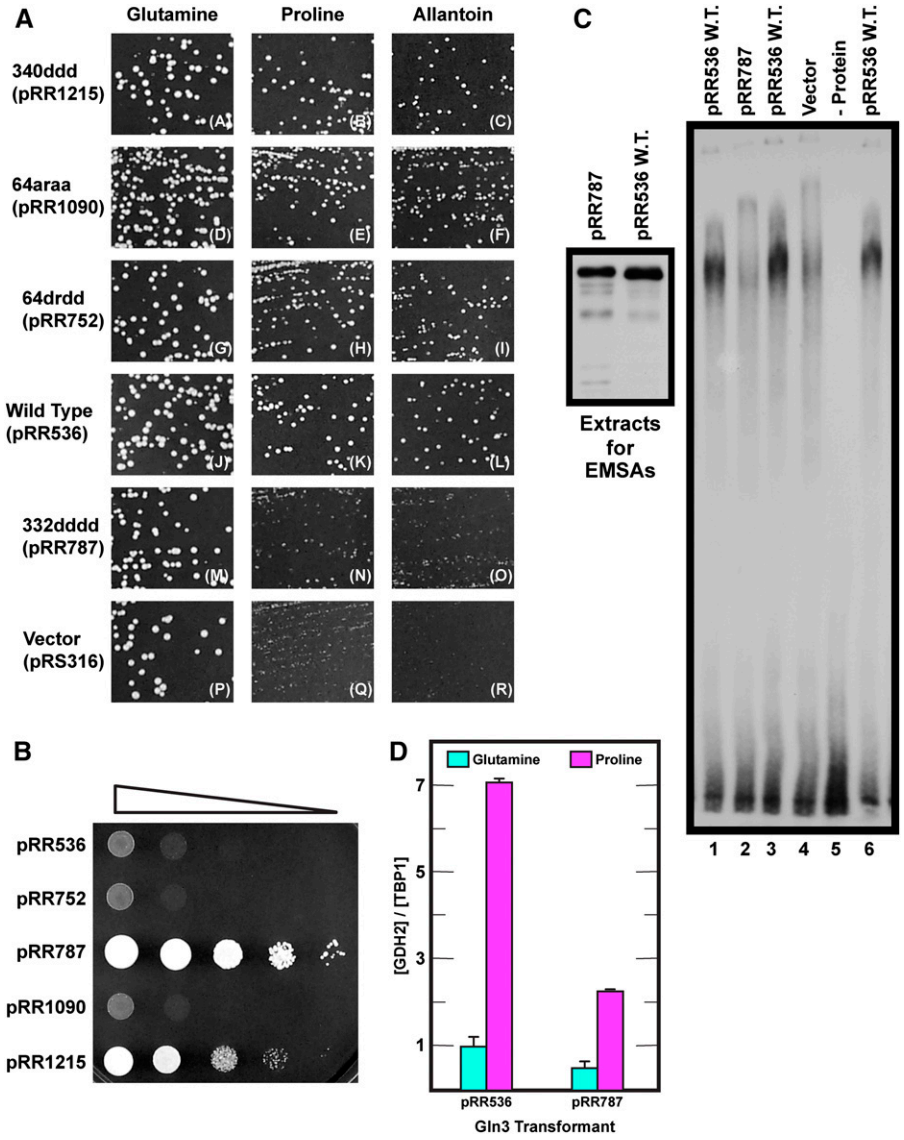

Figure 9 DNA binding is severely damaged or abolished in pRR787. (A) Growth of wild-type (pRR536) and *gln3* substitution mutant plasmids in nitrogen-rich glutamine and nitrogen-poor proline or allantoin media. The indicated plasmids were used to transform *gln3*Δ*gat1*Δ strain FV007. (B) Rapamycin sensitivity of wild-type (pRR536) and *gln3* substitution mutant plasmids. The indicated plasmids were used to transform *gln3*Δ*gat1*Δ strain FV007. Equivalent amounts of the transformant cultures were serially diluted and spotted onto YNB-glutamine medium containing 50 ng/ml rapamycin and grown at 30° for 5.75 days. (C) DNA binding of wild-type (pRR536) and substitution mutant (pRR787) proteins. Protein extracts from YNB-glutamine-grown transformants were used to measure binding between wild-type Gln3-Myc^{13}, 332dddd Gln3-Myc^{13}, and the NCR-sensitive *DAL3* promoter, as described in *Materials and Methods*. *DAL3* promoter oligonucleotide (*DAL3–5*) radiolabeled using the polynucleotide kinase reaction and γ-^{32}P-ATP was used as the probe. Minus protein (-protein) and vector pRS316 (Vector) were used as negative controls. (D) NCR-sensitive *GDH2* transcription is significantly decreased in cells containing Gln3-Myc^{13} that is defective in DNA binding. RNAs from wild-type Gln3-Myc^{13} (pRR536) and Gln3$_{L332D,L336D,M340D,L343D}$-Myc^{13} (pRR787) transformants (FV007 *gln3*Δ, *gat1*Δ recipient) grown in YNB-glutamine *vs.* YNB-proline medium were prepared as described in *Materials and Methods*. *GDH2* transcription was assayed by qualitative RT-PCR.

Therefore, we assayed Gln3-Myc^{13} localization in cells growing in complex SC or minimal YNB-ammonia medium. Note that NCR-sensitive gene expression is repressed in both of these nitrogen-replete media, especially SC medium in the strains we used. As expected, wild-type Gln3-Myc^{13} (pRR536) was highly cytoplasmic in the first medium and substantially so in the second (Figure 10A). Unexpectedly, especially given the response in YNB-glutamine medium, 332dddd Gln3-Myc^{13} (pRR787) responded as the originally reported 336–345 *gln3* deletion (Carvalho and Zheng 2003); it was largely nuclear in SC medium. In YNB-ammonia medium, however, nuclear localization was not nearly as complete (Figure 10A). 64drdd Gln3-Myc^{13} (pRR752) also was nuclear-cytoplasmic or nuclear in SC medium and highly nuclear in YNB-ammonia medium (Figure 10A). Comparing these data with those in Figures 1 and 2, we concluded that medium composition was in fact a critical variable with respect to 332dddd Gln3-Myc^{13} localization.

We further investigated the influence of growth medium composition on Gln3-Myc^{13} localization by comparing its distribution in YNB-glutamine medium, YNB-ammonia medium + casamino acids, and YNB-glutamine medium to which both ammonia and casamino acids were added (Figure 10B). As expected, wild-type Gln3-Myc^{13} (pRR536) was securely sequestered in the cytoplasm of all three of these highly repressive media (Figure 10B). In contrast, 64drdd Gln3-Myc^{13} (pRR752) was constitutively nuclear irrespective of the medium in which the cells were grown. However, 332dddd Gln3-Myc^{13} (pRR787) was largely cytoplasmic in YNB-glutamine medium but highly nuclear in the two other media, both of which were more nitrogen-rich than YNB-glutamine medium alone (Figure 10B). Note that both repressive YNB–casamino acid medium and YNB-glutamine + casamino acid + ammonia medium effectively sequestered wild-type Gln3 in the cytoplasm. Together these data indicated that nuclear Gln3 localization was highly dependent on the

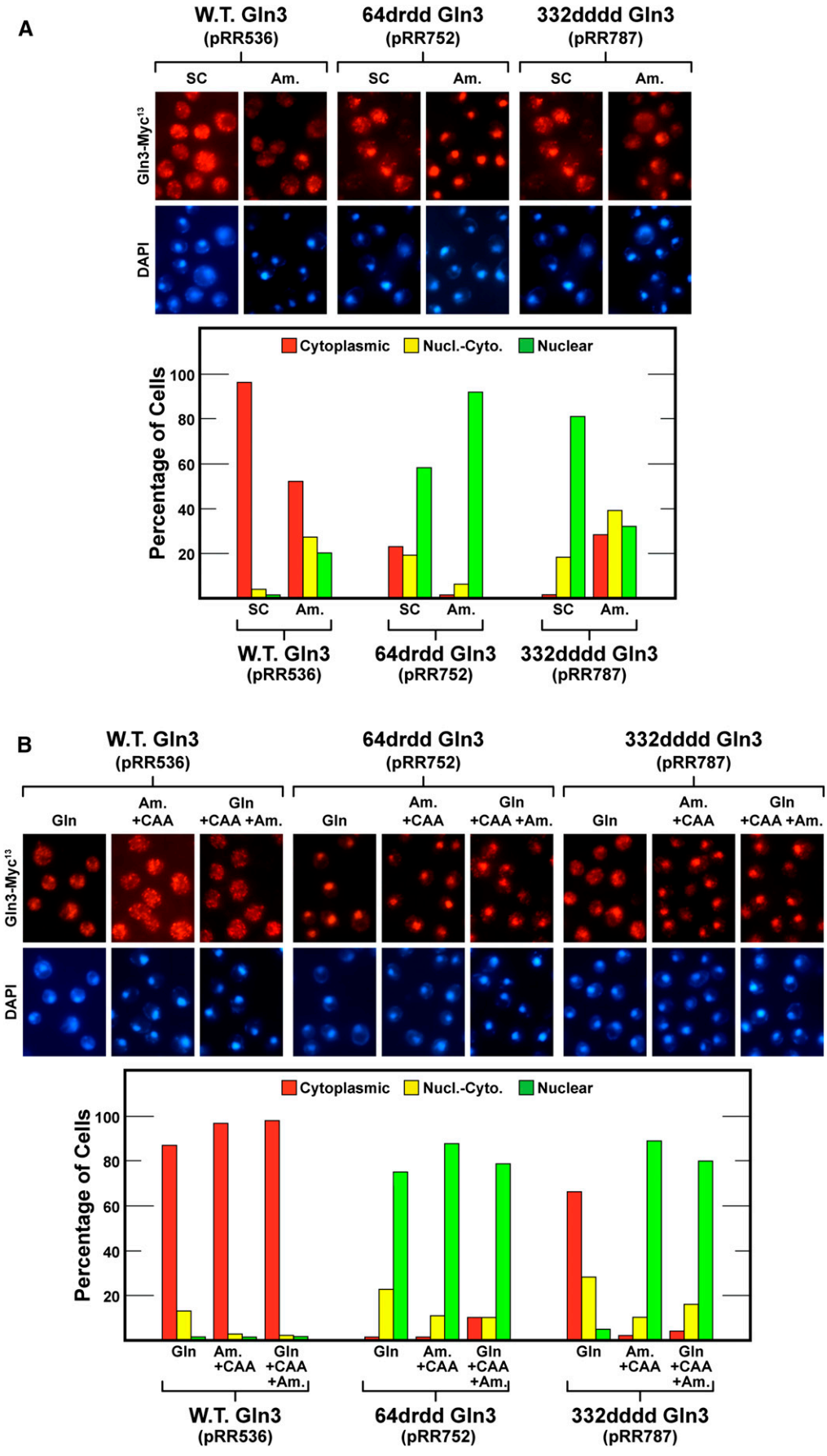

Figure 10 (A) 64drdd Gln3-Myc^{13} (pRR752) and 332dddd Gln3-Myc^{13} (pRR787) nuclear export in cells cultured in repressive complex SC or YNB-ammonia medium. (B) Casamino acids (CAA) and ammonia (Am) inhibit nuclear Gln3$_{64–73}$-dependent export in YNB-glutamine-grown (Gln) cells. All cultures were grown to mid-log phase in medium containing the indicated nitrogen sources before being assayed for intracellular Gln3-Myc^{13} localization, as described in Figure 1, C–E.

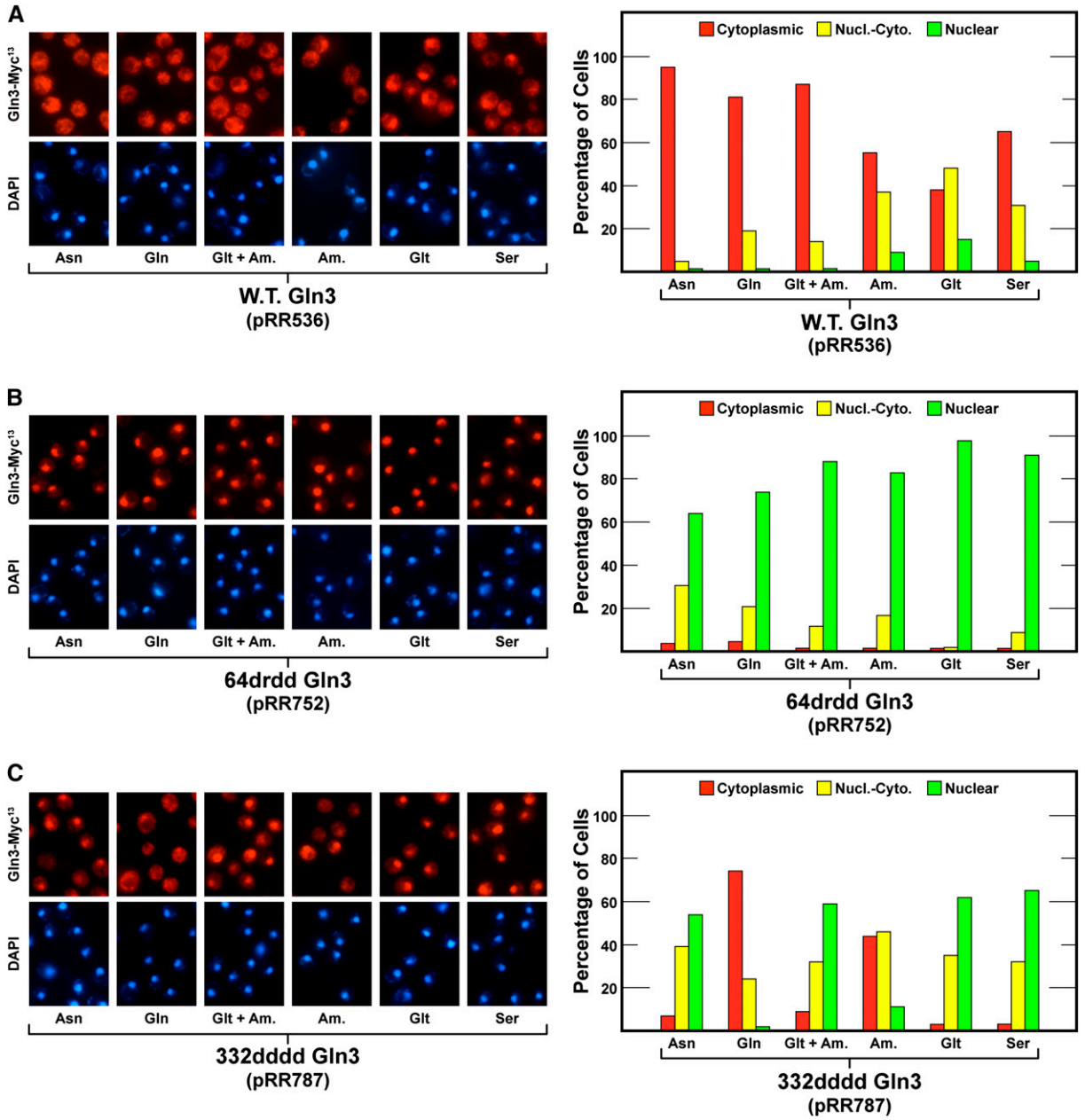

Figure 11 Nuclear Gln3-Myc^{13} export of wild-type Gln3-Myc^{13} (pRR536, panel A), 64drdd Gln3-Myc^{13} (pRR536, Panel B), and 332dddd Gln3-Myc^{13} (pRR787, Panel C) in cells provided with a range of repressive to moderately repressive nitrogen sources. Cells were grown to mid-log phase in YNB medium containing the indicated nitrogen sources (asparagine, Asn; glutamine, Gln; glutamate + ammonia, Glt + Am; ammonia, Am; glutamate, Glt; or serine, Ser) before being sampled for assay of intracellular Gln3-Myc^{13} localization as in Figure 1, C–E.

particular nitrogen source in which the mutant cells were growing. Otherwise, 332dddd Gln3-Myc^{13} (pRR787) would have been highly cytoplasmic in all the media tested.

Nuclear export of 332dddd Gln3-Myc^{13} is specific to glutamine; other repressive nitrogen sources do not support it

The preceding data suggested that the nature of the repressive nitrogen source employed was more important than whether or not it was nitrogen-rich and hence repressive. There was indeed nitrogen-source-dependent specificity to the export of Gln3-Myc^{13} from the nucleus in the 332dddd Gln3-Myc^{13} (pRR787) mutant. To establish this specificity in greater detail, we grew cells containing wild-type Gln3-Myc^{13} (pRR536), 332dddd Gln3-Myc^{13} (pRR787), or 64drdd Gln3-Myc^{13} (pRR752) in YNB medium containing single nitrogen sources ranging from highly to moderately repressive: asparagine, glutamine, ammonia + glutamate, ammonia, glutamate, and serine.

As expected, the first three equally repressive nitrogen sources securely sequestered wild-type Gln3 (pRR536) in the cytoplasm; it was also substantially cytoplasmic with

the remaining three (Figure 11A). Importantly, in all known previous transcriptional studies, glutamate + ammonia has yielded the same results as glutamine alone, not surprisingly, because they are the immediate precursors of glutamine biosynthesis. Positively correlating with previous experiments, 64drdd Gln3-Myc^{13} (pRR752) was constitutively nuclear or largely so irrespective of the nitrogen source provided (Figure 11B). In contrast, 332dddd Gln3-Myc^{13} (pRR787) was highly cytoplasmic when glutamine was provided (Figure 11C). With ammonia, there also was substantial cytoplasmic 332dddd Gln3-Myc^{13} localization, but with the remainder of the nitrogen sources, even those that are highly repressive, *e.g.*, asparagine or glutamate + ammonia, it was substantially nuclear.

Glutamine analogues elicit Gln3 export from the nucleus

These data argued that two distinct sequences influence nuclear localization and export of Gln3-Myc^{13}. Gln3 residues 64–73 (wild type in the 332dddd Gln3-Myc^{13} mutant) appeared to function in a glutamine-dependent manner rather than in response to gross NCR when the Gln3 DNA binding domain was damaged or destroyed, as with 332dddd Gln3-Myc^{13} (pRR787). If the presence of glutamine was indeed specifically responsible for 332dddd Gln3-Myc^{13} export, we predicted that similar export should be observed if glutamine analogues rather than glutamine itself were added to proline-grown cells, where Gln3-Myc^{13} is largely nuclear.

Therefore, we tested a series of amino acid analogues. The first four were well-established glutamine analogues that either substitute for glutamine and/or are effective inhibitors of reactions in which glutamine is a substrate: GAGM substitutes for glutamine in the asparagine synthetase B and γ-glutamylcysteine synthetase reactions (Boehlein *et al.* 1996; Katoh *et al.* 1998). It is also an effective inhibitor, along with other glutamine analogues, of glutamine transport (Jayakumar *et al.* 1987; Low *et al.* 1991; Molina *et al.* 1995) and in the regulation of nitrate reductase (McCarty and Bremner 1992). DON substitutes for glutamine in X-ray crystallographic studies of glutaminase (Thangavelu *et al.* 2014) and is an effective inhibitor of γ-glutamyl transferase, transamidase, and asparagine synthetase activities (Ghosh *et al.* 1960; Milman and Cooney 1979; Payne and Payne 1984). AZA blocks transfer of nitrogen from glutamine to purine precursors (Aaronson 1959). It is also an effective inhibitor of glutamate synthase (GOGAT), a principal reaction along with glutamine synthetase in ammonia assimilation (Kusnan *et al.* 1987; Baron *et al.* 1994; Cogoni *et al.* 1995). DON and AZA both react, forming covalent bonds, with glutamine-dependent enzymes involved in purine and pyrimidine biosynthesis and hence nucleotide synthesis. βAsp is a competitive inhibitor of glutamine in the asparagine synthetase reaction and also competes with asparagine for binding to asparaginyl-tRNA synthetase (Gantt *et al.* 1980). In addition to these glutamine analogues, LEth, MAsp, MGlt, and Msx were included as negative controls.

We grew wild-type (TB123) cells (the strain used in most of our previous work) in proline medium and treated them with each of the inhibitors just mentioned. GAGM, DON, AZA, and βAsp treatment efficiently relocated Gln3-Myc^{13} from the nucleus to the cytoplasm, whereas LEth, MAsp, MGlt, and Msx were without effect or, in the case of LEth, with only a modest effect (Figure 12A). These results were consistent with the idea that high glutamine strongly promoted Gln3-Myc^{13} export from the nucleus.

There was, however, an alternative way that glutamine analogues might have elicited cytoplasmic Gln3-Myc^{13}. Some amino acid analogues inhibit protein synthesis. Such inhibition would result in accumulation of intracellular amino acids, thereby preventing nuclear Gln3-Myc^{13} import. Although a viable possibility, earlier data suggested that the effects of protein synthesis inhibition on Gln3 localization were more drawn out (Tate and Cooper 2013). To directly evaluate this possibility, we compared the time courses of Gln3-Myc^{13} localization in cells treated with either GAGM or high concentrations (200 μg/ml) of cycloheximide. At this concentration, cycloheximide almost instantly inhibits protein synthesis elongation in yeast (Bossinger and Cooper 1976; Cooper and Bossinger 1976). Treating wild-type TB123 or JK9-3da cells containing wild-type Gln3-Myc^{13} (pRR536) with GAGM almost completely relocated Gln3-Myc^{13} from the nucleus to the cytoplasm in 15 min. When the experiment was repeated with cycloheximide, Gln3-Myc^{13} was cytoplasmic in only about 40% of the cells even after 1 hr of treatment (Figure 12B). These results argued that glutamine analogues were unlikely to be eliciting cytoplasmic accumulation of Gln3-Myc^{13} primarily by inhibiting protein synthesis.

Next, we analyzed the effects of the glutamine analogues on the nuclear export of 64drdd Gln3-Myc^{13} (pRR752) and 332dddd Gln3-Myc^{13} (pRR787) in proline-grown cells treated with GAGM or DON (Figure 12C). Neither GAGM nor DON treatment had any effect on nuclear 64drdd Gln3-Myc^{13} (pRR752) localization. This was the expected result because of loss of the NES function. In contrast, the addition of GAGM or DON to cells containing 332dddd Gln3-Myc^{13} (pRR787) resulted in highly cytoplasmic 332dddd Gln3-Myc^{13} localization (Figure 12C).

Addition of additional amino acids to glutamine-grown cells diminishes the ability of glutamine to elicit nuclear Gln3 export

The preceding data raised two paradoxical questions. First, why was glutamine able to elicit Gln3 NES-dependent nuclear Gln3-Myc^{13} export, whereas all the other well-established repressive nitrogen sources (*i.e.*, asparagine, glutamate + ammonia, and SC media) were not? Second, why was ammonia alone, but not ammonia + glutamate, able to elicit moderate 332dddd Gln3-Myc^{13} export? Because ammonia and glutamate are the immediate precursors of glutamine synthesis and enter the cell via different transport systems, the presence of the two of them would *a priori* be expected to

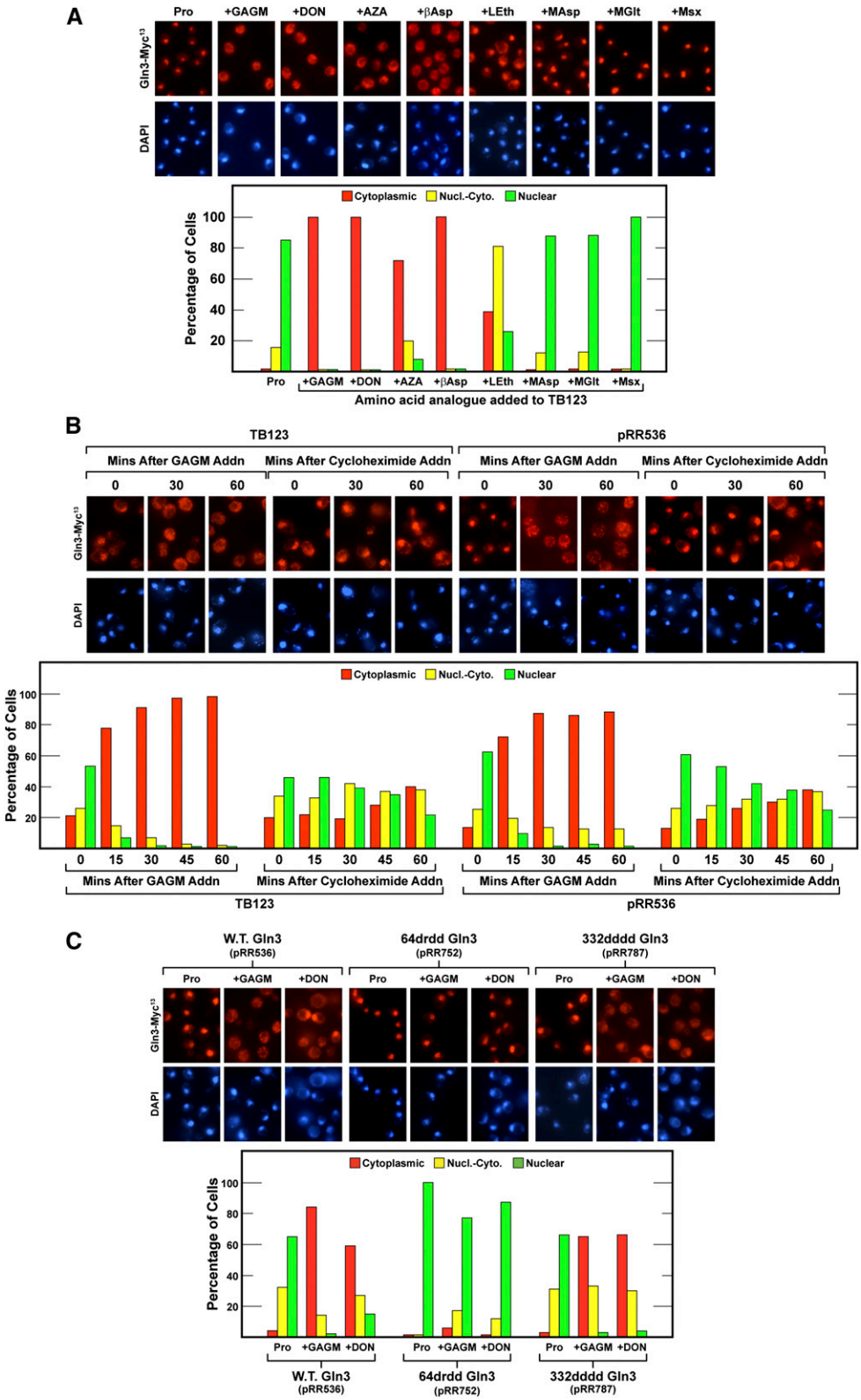

Figure 12 (A) Glutamine analogues elicit the export of wild-type Gln3-Myc[13] from the nuclei of proline-grown cells, a growth condition in which normally Gln3-Myc[13] is highly nuclear. Wild-type TB123 cells were grown to mid-log phase in YNB-proline medium and sampled for Gln3-Myc[13] localization. GAGM, DON, AZA, βAsp, LEth, MAsp, MGlt, or Msx was added and the cells incubated for 30 min before being sampled again for the assay of Gln3-Myc[13] localization. (B) GAGM elicits nuclear Gln3-Myc[13] export much more rapidly than cycloheximide. Wild-type TB123 and transformants (JK9-3da, containing wild-type *GLN3* plasmid pRR536) were grown as described in A. The cultures were sampled and then either 2 mM GAGM or 200 μg/ml cycloheximide was added. Thereafter, the cultures were sampled as indicated for 60 min, and the intracellular distribution of Gln3-Myc[13] was determined as described in Figure 1, C–E. (C) Glutamine analogues GAGM and DON elicit nuclear export of wild-type Gln3-Myc[13] (pRR536), 332dddd Gln3-Myc[13] (pRR787), but not 64drdd Gln3-Myc[13] (pRR752). The experimental format and assay of Gln3-Myc[13] localization were the same as in Figure 12A except that transformants (JK9-3da) containing the wild-type and mutant plasmids were used in place of wild-type strain TB123.

facilitate glutamine synthesis. We reasoned that the answers to both questions were associated with the intracellular flux of glutamine. There are three potential sources of intracellular glutamine: transport into the cytoplasm from the medium, mobilization from the vacuolar stores into the cytoplasm, or *in vivo* synthesis from α-ketoglutarate and ammonia via the intermediate formation of glutamate (Figure 13A). When glutamine is provided as the sole nitrogen source, all other

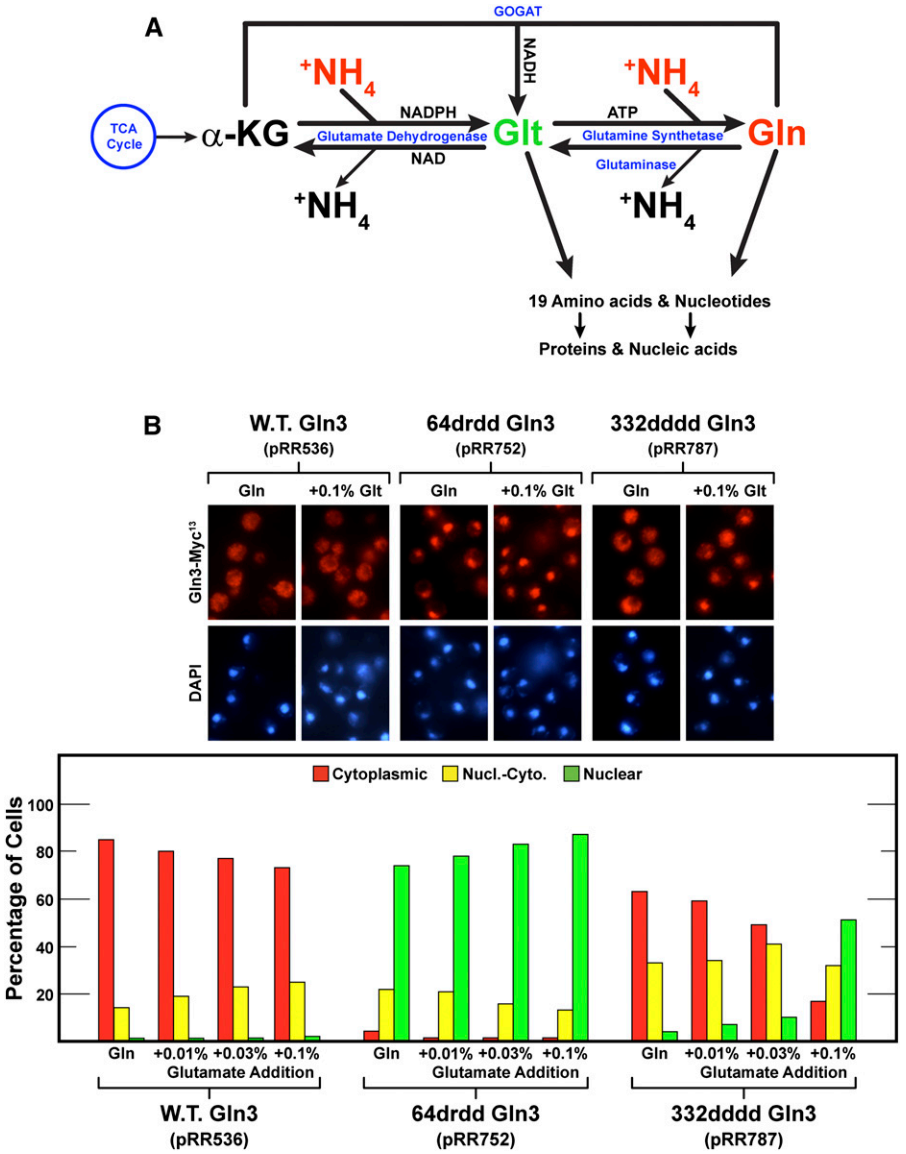

Figure 13 (A) Pathway for the assimilation of ammonia into glutamate and glutamine and the incorporation of these amino acids into other nitrogenous cellular components. (B) Providing an additional means of synthesizing amino acids (added glutamate) inhibits $Gln3_{64-73}$-dependent nuclear 332dddd Gln3-Myc[13] (pRR787) export. Wild-type Gln3-Myc[13] (pRR536) and mutant transformants (pRR752 and pRR787) were grown to mid-log phase in YNB-glutamine (0.1%) plus the indicated amounts (final concentrations) of glutamate medium. Samples of these cultures were then assayed for Gln3-Myc[13] localization as described in Figure 1, C–E.

nitrogenous compounds, *e.g.*, amino acids, nucleotides, and so on, must be synthesized from glutamine. Hence, it is not surprising that cytoplasmic glutamine levels are relatively high in glutamine-grown cells (Figure 13A). The rate of synthesis of protein and other macromolecules will be limited by the amounts of one or more of the other 19 amino acids or nitrogenous precursors being synthesized from glutamine rather than a limitation of glutamine itself. The argument is similar when ammonia is provided as the nitrogen source. The cytoplasmic ammonia level is high, driving the NADPH glutamate dehydrogenase and glutamine synthetase reactions toward the synthesis of glutamine.

However, if alternative routes of acquiring the other 19 amino acids and nitrogenous precursors are provided, as occurs in complex SC medium or the addition of glutamate to YNB-ammonia-grown cells, limitations imposed on the rates of macromolecule synthesis by insufficient supplies of precursors other than glutamine itself are decreased. The increased rates of glutamine incorporation that occur as a result of lifting these limitations concomitantly lowers cytoplasmic glutamine levels relative to what they would be if glutamine or ammonia alone were provided (Figure 13A). An extreme example of this glutamine limitation occurs following the inhibition of glutamine synthetase with Msx.

This reasoning predicted that adding increasing amounts of glutamate to YNB-glutamine medium would decrease 332dddd Gln3-Myc[13] (pRR787) export. We tested this prediction by growing cells in 0.1% glutamine medium containing increasing amounts of glutamate. There was a slight but noticeable decrease in cytoplasmic wild-type Gln3-Myc[13] (pRR536) localization as glutamate additions were increased (Figure 13B). When similar glutamate additions were made to cells containing 64drdd Gln3-Myc[13] (pRR752), nuclear Gln3 localization also increased slightly. Adding increasing concentrations of glutamate to cells containing 332dddd Gln3-Myc[13] (pRR787) at first modestly shifted Gln3-Myc[13]

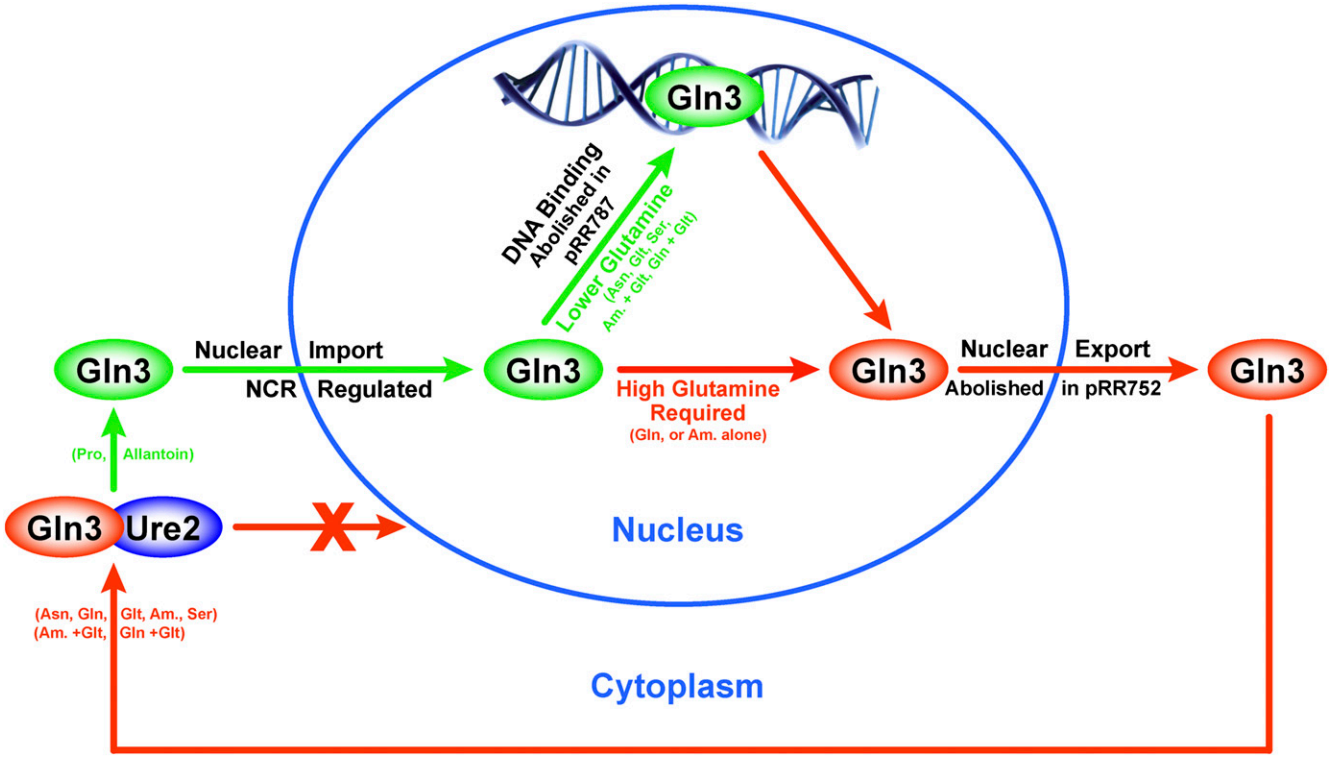

Figure 14 Summary of Gln3 responses to alteration of residues 64–73 (pRR752) or DNA binding site residues 332–345 (pRR787). $Gln3_{64–73}$ is required for nuclear Gln3-Myc[13] export under all growth conditions (pRR752). When intracellular glutamine levels are high, Gln3-Myc[13] can exit the nucleus without binding to its promoter target DNA sequence, *i.e.*, in the absence of a functional Gln3 DNA binding site (pRR787). When glutamine levels are low, Gln3-Myc[13] can exit the nucleus only if the residues required for DNA binding are intact and DNA binding can occur. Repressive nitrogen sources that prevent nuclear Gln3 entry, *e.g.*, asparagine and glutamate + ammonia, are not sufficient to permit nuclear Gln3 export in the absence of a functional DNA binding site.

localization out of the cytoplasm. However, when we increased the glutamate concentration to 0.1%, 332dddd Gln3-Myc[13] (pRR787) export decreased precipitously, with Gln3-Myc[13] remaining largely nuclear (Figure 13B).

Discussion

Data presented in this work indicate that nuclear Gln3 export requires Gln3 residues 64–73, which are homologous in primary sequence and predicted secondary structure to canonical eukaryotic NESs. Rectifying our results with those reporting that Gln3 residues 336–345 function as the Gln3 NES (Carvalho and Zheng 2003), we discovered that deletion of the latter residues destroys both a NES-homologous sequence and the Gln3 zinc finger DNA binding domain. This finding led to the discovery that the level of glutamine itself or a metabolite unique to glutamine and for which glutamine analogues can substitute determines whether Gln3 DNA binding is required for Gln3 to be exported from the nucleus (Figure 14). When Gln3 DNA binding is severely damaged or abolished by altering residues contacting the DNA, export is not observed with a variety of highly repressive nitrogen sources that prevent nuclear Gln3 entry, *e.g.*, asparagine or glutamate + ammonia. Most significantly, and in contrast with other repressive nitrogen sources, Gln3 was effectively exported from the nuclei of glutamine- and, to a limited extent, ammonia-grown cells. Therefore, when cytoplasmic glutamine levels are relatively high, as occurs when glutamine is the sole nitrogen source or glutamine analogues are added to the culture, Gln3-Myc[13] exits from the nucleus in the absence of Gln3 DNA binding (Figure 14). Conversely, when relative cytoplasmic glutamine levels are lowered, as occurs when additionally providing the cells with other equally or less repressive nonglutamine sources (*e.g.*, asparagine and glutamate + ammonia) that are useful nitrogen donors for nitrogenous compound biosynthesis in their own right, Gln3 DNA binding must occur for Gln3 to effectively exit from the nucleus. This reasoning also offers an explanation for why the effects of Msx treatement have been so immune to alterations in Gln3 that affect its localization in response to other perturbations, *e.g.*, rapamycin treatment or NCR. That the observations in this work derive from the regulated operation of nuclear Gln3 export is further supported by the fact that DNA binding is not required for nuclear Gln3 export if an unregulated NES, such as that derived from PKI, is ectopically added to the Gln3 molecule.

Two-tiered regulation of intracellular Gln3 localization

We conclude from these data that overall Gln3 localization is subject to a two-tiered system of regulation. Overall nitrogen availability in the cell, *i.e.*, NCR, regulates nuclear Gln3 entry. In this first tier, when nitrogen sources (*e.g.*, glutamine,

asparagine, ammonia, and casamino acids) that can be readily transported and assimilated are available in sufficient quantity, nuclear Gln3 entry is repressed (Figure 14). As these sources decrease or only poorly transported and/or used sources are available, nuclear Gln3 entry becomes increasingly derepressed. However, we additionally envision, as did Carvalho *et al.* (2001), that Gln3 continuously cycles in and out of the nucleus. Therefore, the intranuclear concentration of Gln3 available to activate NCR-sensitive transcription is determined by the relative rates of its entry and exit. We speculate that in all but the most glutamine-rich environments, it is advantageous for nuclear Gln3 to bind to NCR-sensitive promoters before cycling out of the nucleus (Figure 14).

In addition to NCR, we posit a second tier of Gln3 regulation. When the relative cytoplasmic levels of glutamine or a glutamine-specific metabolite increase sufficiently, *e.g.*, when glutamine or ammonia is provided as the sole nitrogen source or glutamine analogues are added to the cell, this second tier of Gln3 regulation comes into play (Figure 14). Not only is Gln3 entry into the nucleus decreased by NCR, but Gln3 entering the nucleus is also able to exit in the absence of a functional DNA binding domain, *i.e.*, without binding to NCR-sensitive promoters (Figure 14). Even the most repressive nonglutamine nitrogen sources, *e.g.*, asparagine or glutamate + ammonia, are unable to signal imposition of the second tier of regulation, which is the strongest experimental support for its existence. This second tier of glutamine-specific regulation makes sense physiologically because under conditions in which the relative cytoplasmic glutamine levels are sufficiently high, there is little need for nuclear Gln3 to bind to NCR-sensitive promoters prior to cycling out of the nucleus. The operation of a two-tiered regulatory system buffers the intracellular movement of Gln3 and increases the potential of its binding to NCR-sensitive promoters in all but the best of nutritional times. This view of Gln3 regulation also offers an explanation for why treating cells with Msx failed to respond to any of the preceding genetic manipulations of Gln3 or physiological manipulations of the cells. Msx *vs.* rapamycin and repressive nitrogen sources other than glutamine were affecting distinctly different regulatory processes. It also offers an explanation of why Msx treatment effectively elicits nuclear Gln3 localization in cells provided with glutamate + ammonia but not those provided with glutamine (J. J. Tate and T. G. Cooper, unpublished observations).

Two-tiered regulation of Gln3 localization accrues advantages during environmental transitions

It is reasonable to ask what specific advantage is gained by the cell from a twofold fail-safe mechanism that permits Gln3 to exit the nucleus without binding to the DNA. We speculate that the advantages accrue during transitions from repressive to derepressive and derepressive to repressive nitrogen environments. As the nitrogen environment becomes more adverse, NCR-sensitive transcription begins to ramp up. At the same time, however, so too will the transcription and production of the GATA repressors Dal80 and Gzf3/Deh1/Nil2 because their transcription is also activated by Gln3 and Gat1 (Cunningham and Cooper 1991; Daugherty *et al.* 1993; Coffman *et al.* 1995, 1996, 1997; Stanbrough and Magasanik 1996; Rowen *et al.* 1997; Soussi-Boudekou *et al.* 1997; Cunningham *et al.* 2000a,b; Georis *et al.* 2009). These repressors compete with Gln3 and Gat1 for DNA binding (Cunningham *et al.* 1994, 2000a,b; André *et al.* 1995; Stanbrough and Magasanik 1996). Therefore, as the transition to poor nitrogen conditions occurs, the imperative DNA binding of Gln3 before it can exit from the nucleus tilts the balance toward increased Gln3 DNA binding and Gln3-dependent transcription even as GATA repressor (Dal80) production increases (Cunningham *et al.* 2000b). Conversely, when cells encounter the best of nitrogen-rich environments, the ability of Gln3 to exit the nucleus without binding to the NCR-sensitive promoters enhances the repressive effects of the GATA repressors and more effectively and rapidly turns down unnecessary and hence wasteful NCR-sensitive transcription.

The fact that Gln3 can bypass DNA binding and directly exit from the nucleus in glutamine-rich environments implies that its mechanism of exit depends on a change in Gln3 structure, which, in turn, depends on Gln3 DNA binding or its participation in transcriptional activation. Supporting this conclusion is the fact that if one inserts an unregulated NES into the Gln3 sequence, *e.g.*, the mammalian PKI NES described in Figure 2, Gln3 can exit the nucleus in the absence of its DNA binding domain. Recall that Gln3 DNA binding domain residues were replaced by the PKI NES. Correlative circumstantial evidence suggests that the change in Gln3-structure involves its becoming phosphorylated. In conditions in which Gln3 is most nuclear and Gln3-mediated transcriptional activation is greatest, *i.e.*, after treating ammonia-grown cells with Msx, during nitrogen starvation, and in some proline-grown cells, Gln3 is hyperphosphorylated (Figures 1 and 2A in Tate *et al.* 2005; Cox *et al.* 2004a). This, in turn, argues that Gln3 hyperphosphorylation likely occurs in the nucleus prior to its export rather than in the cytoplasm, as previously envisioned. However, much more information about the potential structures of nuclear and cytoplasmic forms of Gln3 is required before these correlations can be substantively considered to reflect cause-effect relationships.

Two caveats to our interpretations merit comment. First, although the data presented in this work provide convincing evidence that Gln3 residues 64–73 are required for its exit from the nucleus, they do not totally eliminate the possibility that the other two candidates, Gln3 residues 10–20 and Gln3 residues 336–345, may function under conditions other than those we employed. One cannot ignore the evidence presented earlier supporting residues 336–345 as being required for this function. The strongest evidence in support of that conclusion was the observation that deleting residues 336–345 abolished the ability of Gln3-Myc^9 to interact with nuclear exportin Crm1 (Carvalho and Zheng 2003). In this regard, it is important to recall, however, that the construct employed in that earlier experiment was an N-terminal Gln3 truncation consisting of Gln3 residues 141–731. Therefore, the

mutant construct lacked both residues 64–73 and residues 336–345 (Carvalho and Zheng 2003). Second is an unavoidable caveat that accompanies the use of glutamine analogues to elicit nuclear Gln3 export. It is the same caveat that applies to all metabolic inhibitors, including rapamycin and Msx. While the inhibitors we used are widely accepted as legitimate glutamine analogues, they affect many enzyme reactions—in fact, any in which glutamine serves as a substrate. Therefore, while they are useful compounds with which to investigate nitrogen regulation in yeast, we attach a prudent level of skepticism to their use and our interpretation of data obtained with them.

Acknowledgments

We thank Thomas Cunningham, William Taylor, and Felicia Waller of the University of Tennessee Molecular Resource Center for providing the DNA sequence and assistance with the qualitative RT-PCR analyses used to verify our mutant constructs. This work was supported by National Institutes of Health National Institute of General Medical Sciences grant GM-35642.

Literature Cited

Aaronson, S., 1959 Mode of action of azaserine on *Gaffkya homari*. J. Bacteriol. 77: 548–551.

André, B., D. Talibi, S. Soussi-Boudekou, C. Hein, S. Vissers *et al.*, 1995 Two mutually exclusive regulatory systems inhibit UASGATA, a cluster of 5′-GAT(A/T)A-3′ upstream from the *UGA4* gene of *Saccharomyces cerevisiae*. Nucleic Acids Res. 23: 558–564.

Arst, Jr., H. N., and D. J. Cove, 1973 Nitrogen metabolite repression in *Aspergillus nidulans*. Mol. Gen. Genet. 126: 111–141.

Baron, A. C., T. H. Tobin, R. M. Wallsgrove, and A. K. Tobin, 1994 A metabolic control analysis of the glutamine synthetase/glutamate synthase cycle in isolated barley (*Hordeum vulgare* L.) chloroplasts. Plant Physiol. 105: 415–424.

Beck, T., and M. N. Hall, 1999 The TOR signalling pathway controls nuclear localization of nutrient-regulated transcription factors. Nature 402: 689–692.

Bertram, P. G., J. H. Choi, J. Carvalho, W. Ai, C. Zeng *et al.*, 2000 Tripartite regulation of Gln3p by TOR, Ure2p, and phosphatases. J. Biol. Chem. 275: 35727–35733.

Binda, M., M. P. Péli-Gulli, G. Bonfils, N. Panchaud, J. Urban *et al.*, 2009 The Vam6 GEF controls TORC1 by activating the EGO complex. Mol. Cell 35: 563–573.

Blinder, D., and B. Magasanik, 1995 Recognition of nitrogen-responsive upstream activation sequences of *Saccharomyces cerevisiae* by the product of the *GLN3* gene. J. Bacteriol. 177: 4190–4193.

Blinder, D., P. W. Coschigano, and B. Magasanik, 1996 Interaction of the GATA factor Gln3p with the nitrogen regulator Ure2p in *Saccharomyces cerevisiae*. J. Bacteriol. 178: 4734–4736.

Boehlein, S. K., S. M. Schuster, and N. G. Richards, 1996 Glutamic acid gamma-monohydroxamate and hydroxylamine are alternate substrates for *Escherichia coli* asparagine synthetase B. Biochemistry 35: 3031–3037.

Bonfils, G., M. Jaquenoud, S. Bontron, C. Ostrowicz, C. Ungermann *et al.*, 2012 Leucyl-tRNA synthetase controls TORC1 via the EGO complex. Mol. Cell 46: 105–110.

Bossinger, J., and T. G. Cooper, 1976 Sequence of molecular events involved in induction of allophanate hydrolase. J. Bacteriol. 126: 198–204.

Broach, J. R., 2012 Nutritional control of growth and development in yeast. Genetics 192: 73–105.

Bysani, N., J. R. Daugherty, and T. G. Cooper, 1991 Saturation mutagenesis of the UAS_{NTR} (GATAA) responsible for nitrogen catabolite repression-sensitive transcriptional activation of the allantoin pathway genes in *Saccharomyces cerevisiae*. J. Bacteriol. 173: 4977–4982.

Cardenas, M. E., N. S. Cutler, M. C. Lorenz, C. J. Di Como, and J. Heitman, 1999 The TOR signaling cascade regulates gene expression in response to nutrients. Genes Dev. 13: 3271–3279.

Carvalho, J., and X. F. Zheng, 2003 Domains of Gln3p interacting with karyopherins, Ure2p, and the target of rapamycin protein. J. Biol. Chem. 278: 16878–16886.

Carvalho, J., P. G. Bertram, S. R. Wente, and X. F. S. Zheng, 2001 Phosphorylation regulates the interaction between Gln3p and the nuclear import factor Srp1p. J. Biol. Chem. 276: 25359–25365.

Coffman, J. A., R. Rai, and T. G. Cooper, 1995 Genetic evidence for Gln3p-independent, nitrogen catabolite repression-sensitive gene expression in *Saccharomyces cerevisiae*. J. Bacteriol. 177: 6910–6918.

Coffman, J. A., R. Rai, T. Cunningham, V. Svetlov, and T. G. Cooper, 1996 Gat1p, a GATA family protein whose production is sensitive to nitrogen catabolite repression, participates in transcriptional activation of nitrogen-catabolic genes in *Saccharomyces cerevisiae*. Mol. Cell. Biol. 16: 847–858.

Coffman, J. A., R. Rai, D. M. Loprete, T. Cunningham, V. Svetlov *et al.*, 1997 Cross regulation of four GATA factors that control nitrogen catabolic gene expression in *Saccharomyces cerevisiae*. J. Bacteriol. 179: 3416–3429.

Cogoni, C., L. Valenzuela, D. González-Halphen, H. Olivera, G. Macino *et al.*, 1995 *Saccharomyces cerevisiae* has a single glutamate synthase gene coding for a plant-like high-molecular-weight polypeptide. J. Bacteriol. 177: 792–798.

Conrad, M., J. Schothorst, H. N. Kankipati, G. Van Zeebroeck, M. Rubio-Texeira *et al.*, 2014 Nutrient sensing and signaling in the yeast *Saccharomyces cerevisiae*. FEMS Microbiol. Rev. 38: 254–299.

Cooper, T. G., 1982 Nitrogen metabolism in Saccharomyces cerevisiae, pp. 39–99 in *Molecular Biology of the Yeast Saccharomyces: Metabolism and Gene Expression*, edited by J. N. Strathern, E. W. Jones, and J. R. Broach. Cold Spring Harbor Laboratory, Cold Spring Harbor, New York.

Cooper, T. G., 2004 Integrated regulation of the nitrogen-carbon interface, pp. 225–257 in *Nutrient-Induced Responses in Eukaryotic Cells* (Topics in Current Genetics Series, Vol. 7), edited by J. Winderickx, and P. M. Taylor. Springer, Berlin.

Cooper, T. G., and J. Bossinger, 1976 Selective inhibition of protein synthesis initiation in *Saccharomyces cerevisiae* by low concentrations of cycloheximide. J. Biol. Chem. 251: 7278–7280.

Cooper, T. G., R. Rai, and H. S. Yoo, 1989 Requirement of upstream activation sequences for nitrogen catabolite repression of the allantoin system genes in *Saccharomyces cerevisiae*. Mol. Cell. Biol. 9: 5440–5444.

Cooper, T. G., D. Ferguson, R. Rai, and N. Bysani, 1990 The *GLN3* gene product is required for transcriptional activation of allantoin system gene expression in *Saccharomyces cerevisiae*. J. Bacteriol. 172: 1014–1018.

Courchesne, W. E., and B. Magasanik, 1988 Regulation of nitrogen assimilation in *Saccharomyces cerevisiae*: roles of the *URE2* and *GLN3* genes. J. Bacteriol. 170: 708–713.

Cox, K. H., J. J. Tate, and T. G. Cooper, 2002 Cytoplasmic compartmentation of Gln3 during nitrogen catabolite repression and the mechanism of its nuclear localization during carbon starvation in *Saccharomyces cerevisiae*. J. Biol. Chem. 277: 37559–37566.

Cox, K. H., A. Kulkarni, J. J. Tate, and T. G. Cooper, 2004a Gln3 phosphorylation and intracellular localization in nutrient limitation and starvation differ from those generated by rapamycin inhibition of Tor1/2 in *Saccharomyces cerevisiae*. J. Biol. Chem. 279: 10270–10278.

Cox, K. H., J. J. Tate, and T. G. Cooper, 2004b Actin cytoskeleton is required for nuclear accumulation of Gln3 in response to nitrogen limitation but not rapamycin treatment in *Saccharomyces cerevisiae*. J. Biol. Chem. 279: 19294–19301.

Crespo, J. L., T. Powers, B. Fowler, and M. N. Hall, 2002 The TOR-controlled transcription activators GLN3, RTG1, and RTG3 are regulated in response to intracellular levels of glutamine. Proc. Natl. Acad. Sci. USA 99: 6784–6789.

Cunningham, T. S., and T. G. Cooper, 1991 Expression of the *DAL80* gene, whose product is homologous to the GATA factors and is a negative regulator of multiple nitrogen catabolic genes in *Saccharomyces cerevisiae*, is sensitive to nitrogen catabolite repression. Mol. Cell. Biol. 11: 6205–6215.

Cunningham, T. S., R. A. Dorrington, and T. G. Cooper, 1994 The UGA4 UAS_{NTR} site required for GLN3-dependent transcriptional activation also mediates *DAL80*-responsive regulation and DAL80 protein binding in *Saccharomyces cerevisiae*. J. Bacteriol. 176: 4718–4725.

Cunningham, T. S., V. V. Svetlov, R. Rai, W. Smart, and T. G. Cooper, 1996 G1n3p is capable of binding to $UAS_{(NTR)}$ elements and activating transcription in *Saccharomyces cerevisiae*. J. Bacteriol. 178: 3470–3479.

Cunningham, T. S., R. Andhare, and T. G. Cooper, 2000a Nitrogen catabolite repression of *DAL80* expression depends on the relative levels of Gat1p and Ure2p production in *Saccharomyces cerevisiae*. J. Biol. Chem. 275: 14408–14414.

Cunningham, T. S., R. Rai, and T. G. Cooper, 2000b The level of *DAL80* expression down-regulates GATA factor-mediated transcription in *Saccharomyces cerevisiae*. J. Bacteriol. 182: 6584–6591.

Daugherty, J. R., R. Rai, H. M. el Berry, and T. G. Cooper, 1993 Regulatory circuit for responses of nitrogen catabolic gene expression to the GLN3 and DAL80 proteins and nitrogen catabolite repression in *Saccharomyces cerevisiae*. J. Bacteriol. 175: 64–73.

Di Como, C. J., and K. T. Arndt, 1996 Nutrients, via the Tor proteins, stimulate the association of Tap42 with type 2A phosphatases. Genes Dev. 10: 1904–1916.

Drillien, R., and F. Lacroute, 1972 Ureidosuccinic acid uptake in yeast and some aspects of its regulation. J. Bacteriol. 109: 203–208.

Drillien, R., M. Aigle, and F. Lacroute, 1973 Yeast mutants pleiotropically impaired in the regulation of the two glutamate dehydrogenases. Biochem. Biophys. Res. Commun. 53: 367–372.

Düvel, K., A. Santhanam, S. Garrett, L. Schneper, and J. R. Broach, 2003 Multiple roles of Tap42 in mediating rapamycin-induced transcriptional changes in yeast. Mol. Cell 11: 1467–1478.

Feller, A., I. Georis, J. J. Tate, T. G. Cooper, and E. Dubois, 2013 Alterations in the Ure2 αCap domain elicit different GATA factor responses to rapamycin treatment and nitrogen limitation. J. Biol. Chem. 288: 1841–1855.

Gantt, J. S., C. S. Chiang, G. W. Hatfield, and S. M. Arfin, 1980 Chinese hamster ovary cells resistant to beta-aspartylhydroxamate contain increased levels of asparagine synthetase. J. Biol. Chem. 255: 4808–4813.

Georis, I., J. J. Tate, T. G. Cooper, and E. Dubois, 2008 Tor pathway control of the nitrogen-responsive *DAL5* gene bifurcates at the level of Gln3 and Gat1 regulation in *Saccharomyces cerevisiae*. J. Biol. Chem. 283: 8919–8929.

Georis, I., A. Feller, F. Vierendeels, and E. Dubois, 2009 The yeast GATA factor Gat1 occupies a central position in nitrogen catabolite repression-sensitive gene activation. Mol. Cell. Biol. 29: 3803–3815.

Georis, I., J. J. Tate, T. G. Cooper, and E. Dubois, 2011a Nitrogen-responsive regulation of GATA protein family activators Gln3 and Gat1 occurs by two distinct pathways, one inhibited by rapamycin and the other by methionine sulfoximine. J. Biol. Chem. 286: 44897–44912.

Georis, I., J. J. Tate, A. Feller, T. G. Cooper, and E. Dubois, 2011b Intranuclear function for protein phosphatase 2A: Pph21 and Pph22 are required for rapamycin-induced GATA factor binding to the *DAL5* promoter in yeast. Mol. Cell. Biol. 31: 92–104.

Ghosh, S., H. J. Blumenthal, E. Davidson, and S. Roseman, 1960 Glucosamine metabolism. V. Enzymatic synthesis of glucosamine 6-phosphate. J. Biol. Chem. 235: 1265–1273.

Görner, W., E. Durchschlag, J. Wolf, E. L. Brown, G. Ammerer *et al.*, 2002 Acute glucose starvation activates the nuclear localization signal of a stress-specific yeast transcription factor. EMBO J. 21: 135–144.

Guthrie, C., and G. Fink, 1991 Guide to yeast genetics and molecular biology. Methods Enzymol. 194: 14–15.

Hardwick, J. S., F. G. Kuruvilla, J. K. Tong, A. F. Shamji, and S. L. Schreiber, 1999 Rapamycin-modulated transcription defines the subset of nutrient-sensitive signaling pathways directly controlled by the Tor proteins. Proc. Natl. Acad. Sci. USA 96: 14866–14870.

Hofman-Bang, J., 1999 Nitrogen catabolite repression in *Saccharomyces cerevisiae*. Mol. Biotechnol. 12: 35–73.

Hynes, M. J., 1975 Studies on the role of the *areA* gene in the regulation of nitrogen catabolism in *Aspergillus nidulans*. Aust. J. Biol. Sci. 28: 301–313.

Jacinto, E., B. Guo, K. T. Arndt, T. Schmelzle, and M. N. Hall, 2001 TIP41 interacts with TAP42 and negatively regulates the TOR signaling pathway. Mol. Cell 8: 1017–1026.

Jayakumar, A., J. S. Hong, and E. M. Barnes, Jr., 1987 Feedback inhibition of ammonium (methylammonium) ion transport in *Escherichia coli* by glutamine and glutamine analogs. J. Bacteriol. 169: 553–557.

Jiang, Y., and J. R. Broach, 1999 Tor proteins and protein phosphatase 2A reciprocally regulate Tap42 in controlling cell growth in yeast. EMBO J. 18: 2782–2792.

Katoh, M., J. Hiratake, and J. Oda, 1998 ATP-dependent inactivation of *Escherichia coli* gamma-glutamylcysteine synthetase by L-glutamic acid gamma-monohydroxamate. Biosci. Biotechnol. Biochem. 62: 1455–1457.

Ko, L. J., and J. D. Engel, 1993 DNA-binding specificities of the GATA transcription factor family. Mol. Cell. Biol. 13: 4011–4022.

Kotaka, M., C. Johnson, H. K. Lamb, A. R. Hawkins, J. Ren *et al.*, 2008 Structural analysis of the recognition of the negative regulator NmrA and DNA by the zinc finger from the GATA-type transcription factor AreA. J. Mol. Biol. 381: 373–382.

Kovari, L. Z., and T. G. Cooper, 1991 Participation of ABF-1 protein in expression of the *Saccharomyces cerevisiae CAR1* gene. J. Bacteriol. 173: 6332–6338.

Kudla, B., M. X. Caddick, T. Langdon, N. M. Martinez-Rossi, C. F. Bennett *et al.*, 1990 The regulatory gene *areA* mediating nitrogen metabolite repression in *Aspergillus nidulans*: mutations affecting specifcity of gene activation alter a loop residue of a putative zinc finger. EMBO J. 9: 1355–1364.

Kulkarni, A. A., A. T. Abul-Hamd, R. Rai, H. El Berry, and T. G. Cooper, 2001 Gln3p nuclear localization and interaction with Ure2p in *Saccharomyces cerevisiae*. J. Biol. Chem. 276: 32136–32144.

Kulkarni, A., T. D. Buford, R. Rai, and T. G. Cooper, 2006 Differing responses of Gat1 and Gln3 phosphorylation and localization to rapamycin and methionine sulfoximine treatment in *Saccharomyces cerevisiae*. FEMS Yeast Res. 6: 218–229.

Kusnan, M. B., M. G. Berger, and H. P. Fock, 1987 The involvement of glutamine synthetase/glutamate synthase in ammonia assimilation by *Aspergillus nidulans*. J. Gen. Microbiol. 133: 1235–1242.

la Cour, T., L. Kiemer, A. Mølgaard, R. Gupta, K. Skriver *et al.*, 2004 Analysis and prediction of leucine-rich nuclear export signals. Protein Eng. Des. Sel. 17: 527–536.

Langdon, T., A. Sheerins, A. Ravagnani, M. Gielkens, M. X. Caddick *et al.*, 1995 Mutational analysis reveals dispensability of the N-terminal region of the *Aspergillus* transcription factor mediating nitrogen metabolite repression. Mol. Microbiol. 17: 877–888.

Low, S. Y., P. M. Taylor, A. Ahmed, C. I. Pogson, and M. J. Rennie, 1991 Substrate-specificity of glutamine transporters in membrane vesicles from rat liver and skeletal muscle investigated using amino acid analogues. Biochem. J. 278: 105–111.

Magasanik, B., and C. A. Kaiser, 2002 Nitrogen regulation in *Saccharomyces cerevisiae*. Gene 290: 1–18.

McCarty, G. W., and J. M. Bremner, 1992 Inhibition of assimilatory nitrate reductase activity in soil by glutamine and ammonium analogs. Proc. Natl. Acad. Sci. USA 89: 5834–5836.

Merika, M., and S. H. Orkin, 1993 DNA-binding specificity of GATA family transcription factors. Mol. Cell. Biol. 13: 3999–4010.

Milman, H.A., and D.A. Cooney, 1979 Partial purification and properties of l-asparagine synthetase from mouse pancreas. Biochem. J. 181: 51–59.

Mitchell, A. P., and B. Magasanik, 1984a Regulation of glutamine-repressible gene products by the GLN3 function in *Saccharomyces cerevisiae*. Mol. Cell. Biol. 4: 2758–2766.

Mitchell, A. P., and B. Magasanik, 1984b Three regulatory systems control production of glutamine synthetase in *Saccharomyces cerevisiae*. Mol. Cell. Biol. 4: 2767–2773.

Molina, M., J. A. Segura, J. C. Aledo, M. A. Medina, I. Núnez de Castro *et al.*, 1995 Glutamine transport by vesicles isolated from tumour-cell mitochondrial inner membrane. Biochem. J. 308: 629–633.

Omichinski, J. G., G. M. Clore, O. Schad, G. Felsenfeld, C. Trainor *et al.*, 1993a NMR structure of a specific DNA complex of Zn-containing DNA binding domain of GATA-1. Science 261: 438–446.

Omichinski, J. G., C. Trainor, T. Evans, A. M. Gronenborn, G. M. Clore *et al.*, 1993b A small single-"finger" peptide from the erythroid transcription factor GATA-1 binds specifically to DNA as a zinc or iron complex (zinc finger/globin gene regulation). Proc. Natl. Acad. Sci. USA 90: 1676–1680.

Orkin, S. H., 1992 GATA-binding transcription factors in hematopoietic cells. Blood 80: 575–581.

Panchaud, N., M. P. Péli-Gulli, and C. De Virgilio, 2013 Amino acid deprivation inhibits TORC1 through a GTPase-activating protein complex for the Rag family GTPase Gtr1. Sci. Signal. 6: ra42.

Payne, G. M., and J. W. Payne, 1984 γ-Glutamyltransferase is not involved in the bulk uptake of amino acids, peptides or gamma-glutamyl-amino acids in yeast (*Saccharomyces cerevisiae*). Biochem. J. 218: 147–155.

Platt, A., T. Langdon, H. N. Arst, Jr., D. Kirk, D. Tollervey *et al.*, 1996a Nitrogen metabolite signalling involves the C-terminus and the GATA domain of the *Aspergillus* transcription factor AREA and the untranslated region of its mRNA. EMBO J. 15: 2791–2801.

Platt, A., A. Ravagnani, H. N. Arst, Jr., D. Kirk, T. Langdon *et al.*, 1996b Mutational analysis of the C-terminal region of AREA, the transcription factor mediating nitrogen metabolite repression in *Aspergillus nidulans*. Mol. Gen. Genet. 250: 106–114.

Powers, T., 2007 TOR signaling and S6 kinase 1: yeast catches up. Cell Metab. 6: 1–2.

Rai, R., F. S. Genbauffe, R. A. Sumrada, and T. G. Cooper, 1989 Identification of sequences responsible for transcriptional activation of the allantoate permease gene in *Saccharomyces cerevisiae*. Mol. Cell. Biol. 9: 602–608.

Rai, R., J. J. Tate, D. R. Nelson, and T. G. Cooper, 2013 *gln3* mutations dissociate responses to nitrogen limitation (nitrogen catabolite repression) and rapamycin inhibition of TorC1. J. Biol. Chem. 288: 2789–2804.

Rai, R., J. J. Tate, K. Shanmuganatham, M. M. Howe, and T. G. Cooper, 2014 A domain in the transcription activator Gln3 specifically required for rapamycin responsiveness. J. Biol. Chem. 289: 18999–19018.

Ravagnani, A., L. Gorfinkiel, T. Langdon, G. Diallinas, E. Adjaji *et al.*, 1997 1997 Subtle hydrophobic interactions between the seventh residue of the zinc finger loop and the first base of an HGATAR sequence determine promoter specific recognition by the *Aspergillus nidulans* GATA factor AreA. EMBO J. 16: 3974–3986.

Rowen, D. W., N. Esiobu, and B. Magasanik, 1997 Role of GATA factor Nil2p in nitrogen regulation of gene expression in *Saccharomyces cerevisiae*. J. Bacteriol. 179: 3761–3766.

Scazzocchio, C., 2000 The fungal GATA factors. Curr. Opin. Microbiol. 3: 126–131.

Shamji, A. F., F. G. Kuruvilla, and S. L. Schreiber, 2000 Partitioning the transcriptional program induced by rapamycin among the effectors of the Tor proteins. Curr. Biol. 10: 1574–1581.

Soussi-Boudekou, S., S. Vissers, A. Urrestarazu, J. C. Jauniaux, and B. André, 1997 Gzf3p, a fourth GATA factor involved in nitrogen-regulated transcription in *Saccharomyces cerevisiae*. Mol. Microbiol. 23: 1157–1168.

Stahl, S. J., and A. M. Gronenborn, 1993 NMR structure of a specific DNA complex of Zn-containing DNA binding domain of GATA-1. Science 261: 438–446.

Stanbrough, M., and B. Magasanik, 1996 Two transcription factors, Gln3p and Nil1p, use the same GATAAG sites to activate the expression of *GAP1* of *Saccharomyces cerevisiae*. J. Bacteriol. 178: 2465–2468.

Stanbrough, M., D. W. Rowen, and B. Magasanik, 1995 Role of the GATA factors Gln3p and Nil1p of *Saccharomyces cerevisiae* in the expression of nitrogen-regulated genes. Proc. Natl. Acad. Sci. USA 92: 9450–9454.

Starich, M.R., M. Wikström, S. Schumacher, H. N. Arst, Jr., A. M. Gronenborn *et al.*, 1998 The solution structure of the Leu22→Val mutant *AREA* DNA binding domain complexed with a TGATAG core element defines a role for hydrophobic packing in the determination of specificity. J. Mol. Biol. 277: 621–634.

Tate, J. J., and T. G. Cooper, 2007 Stress-responsive Gln3 localization in *Saccharomyces cerevisiae* is separable from and can overwhelm nitrogen source regulation. J. Biol. Chem. 282: 18467–18480.

Tate, J. J., and T. G. Cooper, 2013 Five conditions commonly used to down-regulate tor complex 1 generate different physiological situations exhibiting distinct requirements and outcomes. J. Biol. Chem. 288: 27243–27262.

Tate, J. J., R. Rai, and T. G. Cooper, 2005 Methionine sulfoximine treatment and carbon starvation elicit Snf1-independent phosphorylation of the transcription activator Gln3 in *Saccharomyces cerevisiae*. J. Biol. Chem. 280: 27195–27204 [erratum: J. Biol. Chem. 282: 13139 (2007)].

Tate, J. J., A. Feller, E. Dubois, and T. G. Cooper, 2006 *Saccharomyces cerevisiae* Sit4 phosphatase is active irrespective of the nitrogen source provided, and Gln3 phosphorylation levels become nitrogen source-responsive in a sit4-deleted strain. J. Biol. Chem. 281: 37980–37992.

Tate, J. J., I. Georis, A. Feller, E. Dubois, and T. G. Cooper, 2009 Rapamycin-induced Gln3 dephosphorylation is insufficient

for nuclear localization: Sit4 and PP2A phosphatases are regulated and function differently. J. Biol. Chem. 284: 2522–2534.

Tate, J. J., I. Georis, E. Dubois, and T. G. Cooper, 2010 Distinct phosphatase requirements and GATA factor responses to nitrogen catabolite repression and rapamycin treatment in *Saccharomyces cerevisiae*. J. Biol. Chem. 285: 17880–17895.

Tate, J. J., I. Georis, R. Rai, F. Vierendeels, E. Dubois *et al.*, 2015 GATA factor regulation in excess nitrogen occurs independently of Gtr-Ego complex-dependent TorC1 activation. G3 5: 1625–1638.

Thangavelu, K., Q. Y. Chang, B. C. Low, and J. Sivaraman, 2014 Structural basis for the active site inhibition mechanism of human kidney-type glutaminase (KGA). Sci. Rep. 4: 3827.

Urban, J., A. Soulard, A. Huber, S. Lippman, D. Mukhopadhyay *et al.*, 2007 Sch9 is a major target of TORC1 in *Saccharomyces cerevisiae*. Mol. Cell 26: 663–674.

Wang, H., X. Wang, and Y. Jiang, 2003 Interaction with Tap42 is required for the essential function of Sit4 and type 2A phosphatases. Mol. Biol. Cell 14: 4342–4351.

Wen, W., A. T. Harootunian, S. R. Adams, J. Feramisco, R. Y. Tsien *et al.*, 1994 Heat-stable inhibitors of cAMP-dependent protein kinase carry a nuclear export signal. J. Biol. Chem. 269: 32214–32220.

Yan, G., X. Shen, and Y. Jiang, 2006 Rapamycin activates Tap42-associated phosphatases by abrogating their association with Tor complex 1. EMBO J. 25: 3546–3555.

Communicating editor: M. Hampsey